/PHOTOACOUSTIC CHARACTERIZATION OF WHEAT KERNELS/

by

VISWANATHAN VENKATARAMAN

B.Sc., Madurai Kamaraj University, India, 1979
M.Sc., Madurai Kamaraj University, India, 1981
M. Tech., I.I.T., New Delhi, India, 1983

A MASTER'S THESIS

submitted in partial fulfillment of the

requirements for the degree

MASTER OF SCIENCE

Department of Physics

KANSAS STATE UNIVERSITY
Manhattan, Kansas

1985

Approved by:

Ronald D. Lee
Major Professor

TO

PROF. RONALD S. LEE

TABLE OF CONTENTS

		Page
LIST OF TABLES		vi
LIST OF FIGURES		vii
LIST OF GRAPHS		viii
ACKNOWLEDGEMENTS		x
Chapter		
1.	INTRODUCTION	1
	1.1 Thesis Objective	1
	1.2 Classification of Wheat	2
	1.3 Purpose of Grain Grading	3
2.	CRITERIA OF WHEAT QUALITY	5
	2.1 Four Groups of Interest	5
	2.2 Methods for Determining the Quality Criteria	6
	2.2.1 Botanical Criteria	6
	2.2.2 Physical Criteria	7
	2.2.3 Chemical Criteria	10
3.	CURRENT TESTS FOR WHEAT HARDNESS MEASUREMENT	13
	3.1 Wheat Kernel Hardness	13
	3.2 Bolting, Hardness and Flour Yield	14
	3.3 Bird's-Eye View for Hardness Measurements	15
	3.4 Tests for Hardness	17
	3.4.1 Particle Size Index Test	17
	3.4.2 Grinding Resistance Test	18
	3.4.3 Pearlograph Method	19

Chapter		Page

	3.4.4 Brabender Hardness Tester .	19
	3.4.5 Brabender Quadrumat Junior Mill	19
	3.5 Comparison of Testing Methods . .	20
4.	KERNEL STRUCTURE AND MICROSCOPIC STUDY	23
	4.1 Kernel Structure	23
	4.2 Electron Microscopic Studies of the Kernel Structure	24
5.	THEORY OF PHOTOACOUSTIC EFFECT OF SOLIDS	35
	5.1 Introduction	35
	5.2 Rosencwaig-Gersho Theory	38
	5.2.1 The Thermal Diffusion Equations	38
	5.2.2 Temperature Distribution in the Cell	41
	5.2.3 Production of the Acoustic signal	43
	5.3 Special Cases	46
	5.3.1 Optically Transparent Solids	46
	5.3.2 Optically Opaque Solids . .	47
	5.4 Summary	48
6.	DESCRIPTION OF PHOTOACOUSTIC APPARATUS	50
	6.1 General Criteria for a Photoacoustic Set-Up	50
	6.2 Physical Set-Up of Photoacoustic Appartus	54

Chapter Page

7. EXPERIMENTAL RESULTS AND DISCUSSION . . . 58

7.1 Ambient Humidity Conditions for Wheat Samples 58

7.2 Experiments and their Results . . . 59

7.3 Conclusions 109

LIST OF REFERENCES 110

LIST OF TABLES

Table		Page
1	Lens System Currents	33
2	Thermal Properties of Wheat Samples	60

LIST OF FIGURES

Figure		Page
1	Longitudinal Section of Grain of Wheat	21
2	Cross Section View	22
3	A Cross Section of Soft Wheat	26
4	A TEM Picture of Single Starch Cell Embedded in Protein Matrix of Soft Wheat	27
5	SAD of Single Starch Cell of Soft Wheat	28
6	A Cross Section of Hard Wheat Sample from TEM	29
7	A Cross Section of Hard Wheat Sample from TEM	30
8	A TEM Picture of Single Starch Cell Embedded in Protein Matrix of Hard Wheat	31
9	SAD of Single Starch Cell of Hard Wheat	32
10	Illustration of Photoacoustic Effect .	34
11	Cross Sectional View of a Simple Cylindrical Photoacoustic Cell	37
12	Spatial Variation of the Time-Dependent Temperature at the Gas-Sample Interface	40
13	Schematic Representation of the Special Cases for the Photoacoustic Theory of Solids	45
14	Block Diagram of the Experimental Set-Up	53
15	Photoacoustic Cell	55

LIST OF GRAPHS

Graph		Page
1	Plot of PAS vs Chopping Frequency for the Black Paper Sample Using an IR LED	63
2	Plot of PAS vs Chopping Frequency for Five Kernels of Soft Wheat Using Different Coloured LEDs	65
3	Plot of PAS vs Chopping Frequency for Five Kernels of Hard Wheat Using Different Coloured LEDs	67
4	Plot of PAS vs Chopping Frequency for Five Kernels of Soft Wheat Sample Using a Red LED as the Source	69
5	Plot of PAS vs Chopping Frequency for Five Kernels of Hard Wheat Sample Using a Red LED as the Source	71
6	Comparison of Plots of PAS vs Chopping Frequency for a Single and Five Kernels of Soft Wheat Using an IR LED	73
7	Plot of PAS vs Chopping Frequency for Soft Wheat Single Kernels Using an IR LED	75
8	Plot of PAS vs Chopping Frequency for Hard Wheat Single Kernels Using an IR LED	77
9	Plot of PAS vs Chopping Frequency for Soft Wheat Kernels at Different Relative Humidities (RH) Using an IR LED	79
10	Plot of PAS vs Chopping Frequency for Hard Wheat Kernels at Different Relative Humidities (RH) Using an IR LED	81
11	Plot of PAS vs Chopping Frequency for Hard Wheat (RH 30%) Using an IR LED . .	83
12	Plot of PAS vs Chopping Frequency for Time Factor Study (0-7 hrs) for the Rate of Moisture Absorption for a Single Kernel of Soft Wheat (RH 90%) Using an IR LED	85

Graph		Page
13	Plot of PAS vs Chopping Frequency for Time Factor Study (3-15 hrs) for the Rate of Moisture Absorption for a Single Kernel of Soft Wheat (RH 90%) Using an IR LED	87
14	Plot of PAS vs Chopping Frequency for Time Factor Study (0-15 hrs) for the Rate of Moisture Absorption for a Single Kernel of Soft Wheat (RH 90%) Using an IR LED	89
15	Plot of PAS vs Chopping Frequency for Time Factor Study (0-11 hrs) for the Rate of Moisture Absorption for a Single Kernel of Hard Wheat (RH 90%) Using an IR LED	91
16	Plot of PAS vs Chopping Frequency for Time Factor Study (11-38 hrs) for the Rate of Moisture Absorption for a Single Kernel of Hard Wheat (RH 90%) Using an IR LED	93
17	Plot of PAS vs Chopping Frequency for Time Factor Study (1-38 hrs) for the Rate of Moisture Absorption for a Single Kernel of Hard Wheat (RH 90%) Using an IR LED	95
18	Plot of PAS vs Chopping Frequency for Single Kernel of Hard and Soft Wheat (RH 90%) at Constant Frequency 1000 Hz	97
19	Plot of PAS vs Chopping Frequency for Single Kernel of Hard and Soft Wheat (RH 90%) at Constant Frequency 100 Hz	99
20	Plot of PAS vs Chopping Frequency for Single Kernel of Hard and Soft Wheat (RH 90%) at Constant Frequency 10 Hz	101
21	Plot of PAS vs Chopping Frequency for Single Kernel of Hard and Soft Wheat with Different Orientations	103
22	Plot of PAS vs Chopping Frequency for Soft Wheat Flour Using an IR LED . .	105
23	Plot of PAS vs Chopping Frequency for Soft Wheat Flour Using an IR LED . .	107

ACKNOWLEDGEMENTS

The author would like to take this opportunity to express his gratitude for the valuable guidance and constructive criticism given by Prof. Ronald S. Lee and Prof. David L. Wetzel, who supervised this thesis.

The financial support of the Kansas Agricultural Experiment Station and use of the facilities of the Physics Department are gratefully acknowledged.

CHAPTER I

INTRODUCTION

The wheats, one of man's basic foods, are complex, living, dynamic systems that still hold many mysteries. These complexities, increased over the years by man-improved wheat types, are the basis for the many uses of wheat. The most important food use is in the manufacture of flour for making bread, biscuit and pastry products. Wheat is also a source of commercial starch and vital gluten. Wheat starch is used in the food and paper industries, in oil well drilling, as laundry starches, and in other products. Thus, it is no wonder that wheat quality means different things to different people.

The tests to be employed in order to differentiate the different wheat varieties may depend to a large extent upon the specific objectives of the person concerned. The use of a specific method often may be determined by the speed with which information is needed. For example, while exhaustive tests to determine quality of wheat may be desirable, frequently the cereal chemist must use a test that is rapid although it may lack exactness. Bakers may examine samples using much material but plant breeders often want to test characteristics of wheat using only a few kernels.

1.1 Thesis Objective

Among the different factors that determine the gradation of wheat samples, "hardness" is one of the most important. The exact meaning for "hardness" varies, even among those who use it most often (1,2) but a closely related term to it is "strength" (3). The principal value of objective hardness measurements lies in their ability to differentiate between hard or soft wheat. Presently, wheat kernels are mostly graded for hardness from their visual appearance. It is quite possible that a new intermediate hard variety could be classified as soft or a soft variety as hard. This is a problem of real importance to Kansas farmers, who grow new wheat varieties. In order to distinguish between hard and soft varieties, a new technique based on the principle of photoacoustics has been developed.

When a light beam, modulated at some frequency, f, is incident on an absorbing surface enclosed in a sealed cell containing gas, an acoustic signal is produced at the same frequency. The strength of the photoacoustic signal depends on the thermal properties of the absorbing surface and the surrounding gas. In this project, wheat kernels were used as the absorbing surfaces and the differences in the photoacoustic signals from a hard and a soft wheat variety were measured. The major objectives of the project were:

1. Build the photoacoustic cell and the associated electronics.

2. Determine the photoacoustic response of wheat kernels.

(a) 10 - 1000 Hz modulation frequency.
(b) Visible - NIR wavelengths.
(c) Two dissimilar wheat varieties.
(d) Effect of moisture.
(e) Single kernel measurement, if possible.

Details of the technique, apparatus set-up and experiments that have been conducted are discussed in chapter V.

1.2 Classification of wheat

Wheat can be classified in several ways, but the most fundamental distinction is based on the botany of the wheat plant whereas the other classifications deal with the properties of the wheat kernel itself. Percival (4) describes 18 species of wheat, but only a few of these are grown commercially. The wheat kernel consists of an outer covering, the starchy material called endosperm, and the germ from which a new plant would grow. In a general way, wheats are classifed according to (a) the texture of the endosperm, because this characteristic of the grain is connected with the way the grain breaks down in milling, and (b) the protein content, because the properties of the flour and its suitability for different purposes are related to this characteristic (5). For commercial purposes, the common wheats must be classified by other characteristics such as hard or soft, either red or white, and spring or winter habit (6). The official grain standards of the United States for wheat, divide this grain into seven classes and under each class there are several subclasses (7). Under each subclass are the grades from 1 to 5 and sample grades. The seven classes and subclasses are as follows:

Class I Hard Red Spring wheat
(a) Dark Northern Spring
(b) Northern spring
(c) Red Spring

Class II Durum wheat
(a) Hard Durum
(b) Amber Durum
(c) Durum

Class III Red Durum wheat

Class IV Hard Red Winter wheat
(a) Dark Hard Winter
(b) Hard Winter
(c) Yellow Hard Winter

Class V Soft Red Winter wheat
(a) Red Winter
(b) Western Red

Class VI White wheat
(a) Hard White
(b) Soft White
(c) White Club
(d) Western White

Class VII Mixed wheat
This includes all mixtures of wheat which cannot be placed in any of the above classes.

The numerical grades under each class or subclass have definite specifications. These grade specifications vary somewhat for the subclasses of the different classes. Counting all the grades which may be designated under each class and subclass, wheat may be placed under 105 different grade designations (7). Besides these there are the special grades such as: tough wheat, smutty wheat, garlicky wheat, weevily wheat, ergoty wheat and treated wheat. This makes an extensive and complicated grading system that requires special training and experience for people engaged in grading and judging wheat. Some countries such as the United States, Canada, Argentina, and the U.S.S.R have established grain standards for wheat based on such factors as texture (hardness), color, foreign material, broken kernels, moisture and test weight.

1.3 Purpose of Grain Grading

The main purpose of grain grading is to facilitate future trading and protect contracts. The grain standards assume to guarantee only the minimum requirements. In establishing grain standards the two factors that should be kept in mind are as follows:

(1) Very simple standards would fail to meet the trade requirements, and

(2) Very complex standards would be impractical for trading.

Hence, standards must be sufficiently inclusive to meet the trade need, and at the same time sufficiently simple to be practical in trading transactions. Grain standards have been much criticized because they do not indicate with sufficient accuracy the quality desired for milling, but a grading system which would indicate milling quality accurately enough for the operative miller, would be too complex to be practical in trading. The grain standards attempt to indicate quality for milling only in a very general way.

For milling purposes these wheat classes may be placed in three general groups:

(1) the hard wheats,
(2) the soft wheats, and
(3) the durums.

The hard wheats would include the hard red winter, the hard red spring and the hard white. For milling purposes these wheats have certain characteristics in common and to a considerable extent they can replace one another in the milling mixture. Within each class of hard wheats there are many kinds and variations of quality from the milling standpoint. There is often a wider variation in milling quality within a class than between the two classes of hard wheats. The soft wheats include the soft red winter and the soft white. Soft wheats are desirable because of certain inherent characteristics which make them suitable for making flours for specific purposes. What was said about variation within classes of hard wheats applies also to the classes of soft wheats.

In certain respects the grading factors are of distinct help in the operative milling. Experience has shown that the spring wheats as a class have certain characteristics by which they are distinguished (7). The same is true of other classes. Besides this there are for each class and subclass certain grading factors, such as test weight, amounts of damage and foreign material, and the amount of mixture of other classes. The amount of wheat from other classes is important because as a rule, each class or kind of wheat is best milled by itself. Mixture is particularly objectionable when hard and soft wheats are mixed because such wheats differ greatly in milling properties.

In short, grain standards facilitate future trading, protect contracts, and obviate preserving the identity of each parcel of grain. Wheat is appraised throughout the world on the basis of the same general characteristics, regardless of whether or not these factors are incorporated in written statements. Differences in varieties, environment, soil, and many other conditions all influence the composition, quality, and characteristics of wheat. Consideration of all these facts reveal that it is not easy to provide a wheat classification that is satisfactory to producers, merchants, and processors alike, but much progress has been made in this endeavor.

CHAPTER II

CRITERIA OF WHEAT QUALITY

Quality in wheat or flour is a relative term. No sound wheat or flour can be judged either good or poor except in comparison with some specific standard or evaluated for some definite use. Wheat and flour have a number of characteristics by which they may be judged in relation to their intended use. No wheat or flour has all the characteristics that may be desired. It is the preponderance of those which are desired in relation to intended use that determines the relative value.

The quality of wheat is usually judged by its suitability for a particular end-use. Wide inherent differences in wheat quality occur, partly as a result of natural evolution and, during the current century, largely through planned breeding. Environmental factors during growth also have a profound influence on wheat quality, often a greater influence than the inherent factors (8). Physical and chemical differences are strikingly great between different lots and varieties of wheat. These differences have far-reaching effects and become the basis for what is loosely referred to as quality (9,10). Actual quality of wheat is due to the cumulative effect of soil, climate, and seed stock on the wheat plant and the kernel components.

2.1 Four Groups of Interest

Wheat is usually studied and evaluated as a class or a variety. For commercial grading purposes wheats are divided into several classes such as hard red winter, soft red winter or hard red spring each having well recognized physical characteristics. Within these classes are grouped the varieties which are more or less similar in cultural characteristics, and are differentiated by heredity as well as by certain characteristics. A wheat class or more particularly a variety may be evaluated as to quality in relation to four groups or interests :

(1) The grower requires good cropping and high yields. He is not concerned with quality (provided the wheat is "fit for milling" or "fit for feeding") unless he sells grain under a grading system associated with price differentials.

(2) The miller requires wheat of good milling quality - fit for storage, and capable of yielding the maximum amount of flour suitable for a particular purpose.

(3) The baker requires flour suitable for making, for example, bread, biscuits or cakes. He wants his flour to yield the maximum quantity of goods which meet the rigid specifications, and therefore requires raw materials of suitable and constant quality.

(4) The consumer requires palatability and good appearance in the goods he purchases; they should have high nutritive value and be reasonably priced.

These criteria are dependent largely on environment - soil, climate and manurial or fertilizer treatment. Within the limits of environment, quality is influenced by characteristics that can be varied by breeding, and is further modified during harvesting, farm drying, transport and storage.

2.2 Methods for Determining the Quality Criteria

Cereal chemists for more than 100 years have been looking for objective methods to determine wheat and flour quality. Many tests have been proposed including those performed on the grain, whole wheat meal, flour, gluten, fermenting flour doughs, and the baked loaf. Some require little sample preparation and simple equipment whereas others require extensive preparation and elaborate equipment. The tests to be employed may depend to a large extent upon the specific objectives of the cereal chemist. The examination of car lots of wheat for grade, color, test weight, variety, insect damage, and soundness prior to purchase or binning is quite different from the testing of varieties for their baking potential. Other chemists may be interested in quality control within one mill or within a given organization. Still others may be interested in purchasing supplies of flour to meet specific requirements. The use of a specific method often may be determined by the speed with which the information is needed. While exhaustive tests to determine quality of wheat may be desirable, frequently the cereal chemist must use a test that is rapid although it may lack exactness. Bakers may examine samples using much material but plant breeders often want to test characteristics of wheat using only a few kernels.

In this project, most of the measurements involved a single or a few wheat kernels, hence only the methods that use the whole wheat kernels will be described in detail while the other methods will be mentioned very briefly.

2.2.3 Botanical Criteria

A. Species

Of the fifteen recognized species of wheat (11), only three (Common wheat, Club and Durum wheats) are of commercial importance in North America. The quality characteristics of the grain of these three species differ considerably and these differences are reflected in the uses made of the milled products. The external physical characteristics of the kernels also differ sufficiently so that grain inspectors ordinarily have no difficulty in species identification.

B. Varieties

Numerous varieties of each species of wheat are recognized and new ones are constantly being developed and released. Yield and resistance to diseases and insect attack are the properties that usually receive the greatest attention in wheat-breeding work, but in recent years increasing emphasis has been placed on the quality of the grain for processing, specifically the milling and the baking quality. Although variety is an important factor influencing wheat quality, wheat is seldom marketed on the basis of individual variety. It is common practise to segregate wheat as it comes to the market according to class, each class consisting of a group of varieties of somewhat similar characteristics and generally used for similar purposes.

2.2.2 Physical Criteria

A. Weight per Unit Volume

One of the most widely used and simplest criteria of wheat quality is the weight of the wheat per unit volume. In the United States and Canada this is expressed in terms of lb. per bu. and in most countries using the metric system, in terms of kg. per hectoliter. The basic factors that affect the weight per unit volume of grain have been discussed by Hlynka and Bushuk (12). They have shown that contrary to popular opinion, kernel size, as such, has little if any influence on test weight. Kernel shape and uniformity of kernel size and shape are important factors influencing test weight, inasmuch as they affect the manner in which the kernels orient themselves in a container. The other important factor influencing the test weight is the density of the grain. Density, in turn, is influenced by the biological structure of the grain and its chemical composition, including its moisture content. Weight per unit volume is an important factor in all wheat grading systems. Its importance lies primarily in the fact that it is at least a rough index of the yield of flour that can be obtained. The average test weight per bu. of U.S. wheat is about 60 lb., but test weights up to 64 lb. are not uncommon. Badly shriveled wheats may have test weights as low as 45 lb. or less.

B. Kernel Weight

Kernel weight, usually expressed in terms of weight per 1,000 kernels, is a function of kernel size and kernel density. Inasmuch as large, dense wheat kernels normally have a higher ratio of endosperm to nonendosperm components than do smaller, less dense kernels, one might expect that kernel weight would be more reliable than test weight as a guide to flour yield. The range in weight per 1,000 kernels for U.S. hard red winter and hard red spring wheat is normally from about 20 to 32 g. For soft red winter, white, and durum wheat the range is normally from about 30 to about 40 g. and the average about 35g.

C. Kernel size and Shape

Kernel size, of course, is closely related to kernel weight and would be expected to be a factor affecting flour yield. Shuey (13) has developed a procedure for sizing wheat according to average cross-sectional area. Three sizes of wire-mesh sieves are used and the percentage of wheat kernels that will not pass endwise through each sieve is determined; predicted milling yield is then calculated by a mathematical formula. In a latter study Shuey and Gilles (14) found evidence that in many cases separating small wheat kernels from large kernels and milling the two fractions separately may lead to greater efficiency in commercial milling operations.

D. Kernel Hardness

Wheat hardness is defined as resistance of kernels to deformation by outside force. Wheat hardness is considered to be an important quality characteristic throuhout the world. In the three major wheat exporting countries, Australia, Canada and the United States, considerable attention is given to segregating wheat on the basis of hardness, and consequently terms such as Australian Prime Hard and US Hard Winter are now common. Of the numerous tests that have been used for hardness, most of them have an abrasive, crushing, grinding, or cutting action. Those selected for interlaboratory work should be sturdy,rapid, and simple to operate. In addition they should lend themselves to standardization, so that results among laboratories agree. The various techniques that are presently being adopted in testing the wheat hardness are elaborately described in Chapter III.

E. Vitreousness

The endosperm texture may be vitreous (steely, flinty, glassy, horny) or mealy (starchy, chalky). Samples may be entirely vitreous or entirely mealy, or may consists of a mixture of both,with one type predominating. The vitreousness of wheat kernels is often considered in connection with apparent hardness in the classification of wheat for grading purposes. Vitreousness is associated with high protein content, but it is strictly a subjective factor and can be considered as only a rough index of protein content.

F. Color

From the color standpoint wheat is classed as either red or white, depending on the color of the bran. These two basic colors, as well as certain variations within each color, are commonly considered in the classfication of wheat for grading purposes. The basic colors are strictly varietal characteristics, but variations within each color are frequently due to environmental factors.

G. Damaged Kernels

Wheat may be damaged from many different causes occuring in the field before harvest, during harvesting or artificial drying operations, or during subsequent storage or handling. When such a damage is recognized during physical examination and is of a type and extent that will decrease storage or processing value, it is considered in grading or otherwise assessing the quality of wheat.

H. Impurities

The quantity and character of impurities or extraneous matter in wheat are obviously important criteria of quality. Most of such material is removed from the wheat in the mill as screenings which are of value in animal feeds. The screenings, however, are of considerably less value than the the wheat on a weight basis.

I. Besatz

Besatz in wheat is considered to be all material other than sound, plump, whole kernels of wheat of the class under consideration. In terms of the U.S. standards, Besatz might be said to include dockage, foreign material, damaged kernels, shrunken and broken kernels, and wheat of other classes. It is not possible, however to determine Besatz in accordance with the ICC (International Association for Cereal Chemistry) system by using the factors in the U.S. Standrds, since the prescribed methods for determining various components of Besatz are not the same as those for determining the corresponding factors in the U.S. Standards.

J. Milling Quality

Most of the physical criteria discussed above are based on relatively simple examinations or tests and are of value inasmuch as they reflect in some degree the milling quality of the wheat or the baking quality of the flour milled from the wheat. Experimental milling, which provides small quantities of flour, is performed to provide information concerning the physical behaviour of the grain during the milling operation and/or to provide flour for obtaining information related to baking characteristics of the resulting flour. Testing wheats for their milling quality is done with respect to such factors as tempering, amount of sizing stock, amount of power required to reduce the middling stocks, hardness, compatability in blends with other wheats, flour yield, and ash and color of the resulting flour.

H. Gluten Washing

When a flour-water dough is manipulated in a volume or stream of water, the starch is washed away and a cohessive mass of gluten is obtained. The quantity and quality of gluten can be evaluated subjectively by an experienced operator, or objectively with any one of several different instruments. Since gluten cannot be obtained easily from whole wheat meal, most workers prefer to use flour.

2.2.3 Chemical Criteria

A. Moisture Content

Moisture content is one of the most important factors affecting the quality of wheat. Since the amount of dry matter in wheat is inversely related to the amount of moisture it contains, moisture content is of direct economic importance. Much of the wheat marketed in the united States contains about 14% moisture, although in the drier areas or in dry seasons the moisture content may be as low as 8%. Of even greater significance is the effect of moisture on the keeping quality of wheat. Dry, sound wheat can be kept for years if properly stored, but wet wheat may spoil completely within a few days. Under practical storage conditions moisture content is usually the principal factor governing the keeping quality of wheat, but factors other than moisture may also have marked effects on storage behavior. Wheat that is too dry also has some disadvantages. Very dry wheat tends to be brittle and to break easily in commercial handling operations. Another disadvantage is that it is some times more difficult to temper it properly to the moisture level required for milling.

The basic method for determining moisture in wheat is usually considered to be the 130° C. 1-hr. air-oven method (14,15). Results obtained by this method have been found by Hart and Neustadt to agree closely with those obtained by the Karl Fischer method (16), considered to be the most accurate available method for determining true moisture content. For most purposes electric moisture meters, based either on the electrical conductance or the capacitance principle, are usually used to determine the moisture content of wheat. These meters are of great practical value, particularly in routine inspection work, because with them moisture determinations can be made very quickly.

B. Protein Content

Protein content in wheat varies from about 6% up to about 20%, depending in part on variety and class but more largely on environmental factors during growth. Abundant rainfall during the period of kernel development usually results in low protein content, whereas dry conditions during that period favor high protein content. Protein content is also influenced considerably by the available soil nitrogen.

Protein content of wheat is ordinarily determined by the well-established Kjeldahl procedure (9) or one of its various modifications. Actually, this method measures organic nitrogen which can be corrected to protein content, based on the average nitrogen content of the proteins in flour (17). This method is reliable, rapid, well adapted to routine work, and the most widely used and accepted test for wheat and flour quality. Its disadvantages, particularly for the small laboratory, are the time, skillful operation, and expensive equipment it requires.

C. Protein Quality

An entirely different concept of wheat protein quality is involved with the physical rather than the nutritional characteristics of bread and other end-products of wheat. It is known that wheats of the same protein content will produce flours which behave quite differently in baking operations, and that in many instances these differences are attributable to qualitative differences in the gluten proteins. Gluten quality is largely a varietal characteristics, although it has been found that excessively high temperatures and low relative humidity during the period when wheat is maturing in the field may have a marked deleterious effect on the quality of the gluten. The wheat-meal fermentation-time test, or dough-ball test and the sedimentation test are the two widely used tests for estimating potential bread-baking strength. The sedimentation test requires much less time than the other one and, because of its greater objectivity, better agreement among replicate tests can usually be obtained.

D. Alpha-Amylase Activity

As previously stated, rainy weather after wheat has matured in the field but before it is actually harvested may cause some of the kernels to sprout. Such kernels have a very high alpha-amylase activity. Even if visible sprouting does not occur, the alpha-amylase level can be considerably elevated as a result of a wet harvest season. Thus the alpha-amylase activity of wheat cannot be reliably estimated by determining the percentage of sprouted kernels.

E. Crude Fiber and Ash

Both crude fiber and ash content of wheat are related to the amount of bran in the wheat and hence have rough inverse relationships to flour yield. Small or shriveled kernels usually have more bran on a percentage basis and therefore more crude fiber and ash, and yield less flour than large plump kernels.

CHAPTER III

CURRENT TESTS FOR WHEAT HARDNESS MEASUREMENT

3.1 Wheat Kernel Hardness

Hardness and softness are milling characteristics relating to the way the endosperm breaks down. It has been observed that, if the cut surface of hard wheat is lightly and uniformly wetted and allowed to dry, a pattern of cracks appears, following the lines of the endosperm cell boundaries. When soft wheat is treated similarly, the pattern of cracks produced bears no relationship to the cellular structure of the endosperm. but passes indiscriminately through the cells. This phenomenon suggests a pattern of areas of mechanical strength and weakness in hard wheat, but fairly uniform mechanical weakness in soft wheat.

Grain kernel hardness is a characteristic very often used in wheat classification. The miller knows that harder wheat usually produces a higher extraction of flour of suitable color. Hard wheat mills to a flour with a higher percentage of damaged starch. Hard wheats yield coarse, gritty flour, free-flowing and easily sifted, consisting of regular-shaped particles, which are mostly whole endosperm cells; soft wheat gives very fine flour consisting of irregular-shaped fragments of endosperm cells, with some flattened particles, which adhere together, sift with difficulty, and tend to close the aperture of sieves. The endosperm of hard wheats may be flinty or mealy in appearance, but its breakdown is always typical of a hard wheat. It is probable that the strength of the protein bonds determines the nature of the breakdown.

Hardness affects the ease of detachment of the endosperm from the bran. In hard wheats the endosperm cells come away more cleanly and remain more intact, whereas in soft wheats the peripheral endosperm cells tend to fragment, part coming away while part is left attached to the bran. The granularity of flour gives a measure of the relative hardness of wheats, the proportion of the flour passing through a fine flour silk decreasing with increasing hardness. Hardness and vitreosity are the most important quality parameters in the marketing of wheat, since they affect its appearance as well as its milling and baking behavior. In many wheat growing countries, vitreousness is used as a means of segregating high protein, hard wheat types by visual appearance. Opaqueness, on the other hand, is traditionally associated with softness and low protein content. The resulting segregates, besides being more uniform in appearance, are also more uniform in their milling characteristics. However, contrary to popular belief, kernel hardness and vitreosity are not due to the same fundamental cause, although it is certainly true that hard wheats are usually vitreous, while soft wheats are rarely so.

3.2 Bolting, Hardness, and Flour Yield

Although hardness can be determined by independent physical tests, it can be evaluated more accurately when determined as a part of the experimental milling test. Unusually hard or soft milling characteristics will usually be reflected in lower flour yields which in turn are evaluated in relation to the wheat to flour protein conversion and ash contents. A wheat that is too hard usually will require more power and more than the normal number of break and reduction operations. The flour from such wheat will usually have a relatively high ash content. If a wheat is too soft, bolting properties will probably be unsatisfactory. Bolting properties are referred to as the way by which the kernels are going to break away during the process of milling. For example, certain stocks will tend to ball-up and not pass through the sieves or will require more sifting time. In addition, the mill flow will be altered as a result of an unusually high quantity of break flour.

Although wheat hardness is associated with high-protein, vitreous wheat, hardness in itself is not an attribute sought by plant breeders. Neither is it welcomed by millers, because unusually hard wheat requires significantly more power to mill and causes more roll repairs and sieve replacements than normal wheat. On the other hand, wheat that is too soft may have poor bolting properties and require longer time for sieving. For economic reasons, therefore, millers should be interested in reliable, quick, simple methods to determine wheat hardness that would be applicable to plant operations. Some plant breeders also interested in such methods to test the hardness of new crosses, especially those between hard and soft wheat varieties.

Kernel hardness or apparent hardness in wheat has been measured for decades using different methods based on different principles. Early researchers had an appreciation of the relationship between grain texture and quality (18,19). Lacking a sophisticated means for evaluating kernel hardness, Biffin (19) employed a visual method. He realized, however, that the translucency or vitreosity was not necessarily related to bread quality. He saw that some soft wheats were translucent, questioned whether such wheats were intrinsically valuable for breadbaking, and declared that the only true test of quality was to bake bread. He was also an early cereal chemist, suggested that wheat be tested for hardness by crushing grain on an iron plate, stating "weak grain...breaks to fine powder while strong grain crushes to angular fragments or to a gritty powder." Following this principle, Cutler and Brinson (1935) developed a procedure for obtaining a particle size index

(PSI)value for wheat.

Since these early efforts, a large body of literature has been developed that bears on procedures to conduct a kernel hardness test, on the genetic aspects of hardness, and on the relation of hardness to variety and to grain moisture content.

3.3 Bird's-Eye View for Hardness Measurements

Chewing wheat to determine hardness was perhaps the most primitive test to determine wheat quality. Taylor, Bayles, and Fifield (20) adapted a Strong-Scott barley pearler to determine objectively the hardness of wheat varieties and of the same varieties grown under different environments. The test consisted of grinding 20 g. of wheat in a barley pearler for one minute. The harder the wheat the smaller the amount of material removed. This ranged from 30% for hard wheat to 60% for soft wheats. McCluggage (21) found that kernel hardness as measured by the pearling test was influenced mostly by variety and less by location and season. Bayles (22) stated that the test was useful to differentiate between soft and hard wheat, and Swanson (23) concluded that hardness was one of the factors to be considered in judging the wheat for baking. Though widely used in soft wheat laboratories, the pearling test has not received wide acceptance for evaluating hard wheat.

Berg, a Swedish investigator (24) , studied the relation of grittiness to variety. The amount of flour retained on a standard sieve when using a specified milling procedure was employed as an indicator of the grittiness of the flour. He concluded that grittiness was a varietal characteristic with no correlation between grittiness and protein content. Cutler and Worzella (25) found a significant positive correlation between the wheat meal fermentation time and the number of vitreous kernels. This suggests, in contrast to the conclusions of Berg, that there is a relationship between protein content and hardness.

The MIAG Micro Hardness Tester measures hardness in grain. Essentially it is a penetrometer and produces an impression on the surface of a thin section of kernel sliced by a microtome. The depth of the indentation provides a measure of kernel hardness. This instrument was used by Grosh and Milner (26), who observed that endosperm hardness decreased with higher moisture content upon tempering.

The Barcol Impressor, similar in principle to the MIAG Tester was used by Katz et al. (27) to determine the hardness of single wheat kernels. This instrument and the MIAG, although satisfactory for research, probably would not be used for routine work by control laboratories because of the time required for sample preparation and testing.

Recently, the Brabender hardness tester (BHT), developed in Europe to evaluate barley malt, has been used to determine hardness of wheat. This tester is a dynamometer coupled to a burr mill which grinds the kernels. A recorder is attached, and graphs of the torque produced during milling are made. The height of the curve recorded on the graph paper indicates hardness.

A brief summary of apparatus and methods for testing wheat hardness is given below. Some of the important testing procedures are discussed in more detail in sections 3.4.1-3.4.5.

A. Apparatus

(1) Brabender Hardness Tester.
(2) Strong-Scott wheat pearler, model 38.
(3) MSA-Whitley particle size analyzer.
(4) Motomco moisture meter.
(5) Ro-tap shaker or any standard flour sifter.
(6) U.S.No. 100 woven-wire cloth sieve.
(7) Udy Protein Analyzer or Kjeldahl nitrogen apparatus.

B. Methods

(1) Average flour particle diameter. Method 50-10, Particle Size Distribution of Flour, Cereal Laboraty Methods (28).
(2) Protein content. Methods 46-11 and 46-14, Crude Protein by Kjeldahl and Udy methods, Cereal Laboratory Methods (28).
(3) Moisture Content. Motomco moisture meter method.
(4) Total flour surface area (TFSA) in sq.m. :

Procedure A:
$TFSA = \text{Flour Yield } (\%) * 4\pi r^2/(4/3)\pi r^3$
where r = radius in microns;
p = density of flour (1.44)

Procedure B: Number of flour particles per g. (n) determined with a counting chamber.

$TFSA = (4\pi r^2 n/10^{12}) * \text{flour yield } (\%)$

where 10^{12} = sq. microns/sq. m. flour.

(5) Flour Yield: meal from the BHT is sieved on a U.S.NO. 100 woven-wire cloth sieve for 15 min. in a Ro-tap shaker. The weight of flour (g.) is the percent yield, since 100 g. of wheat is milled.
(6) Wheat hardness index: Wheat-hardness peak

(curve height) divided by percent flour yield. (The percent bran is ignored because it complicates total surface area measurements and detracts from the sensitivity of the tests as measured by correlation coefficients.)

(7) Wheat pearling index: the percent of material pearled from 20 g. of wheat in 42 sec.

(8) Wheat hardness peak: Maximum height of the BHT graph.

(9) Wheat mellowness: the inverse of hardness determined by measuring width of BHT curve.

In summary, flour yield, total flour surface area, and protein and moisture contents are important factors in wheat hardness measurements. In addition, unknown factors such as complex physical interactions between protein, starch, minerals, and moisture within the endosperm matrix during maturation might have significant effects on kernel hardness. Even the bran, which proteots the endosperm, is probably a factor. The hardness peak is a measure of the work required to grind 100 g. of wheat. When this value was divided by the percent flour, the quotient was a factor named the wheat hardness index. This value correlated highly with protein content per sq. m. of flour where protein acts as a cohessive agent binding the endosperm particles together and thus making them more resistant to milling.

3.4.1 Particle Size Index Test

In the PSI test, the Labconco Heavy Duty Mill, equipped with special burrs, is calibrated (29). Grain (20 g.) is ground by passing through the grinder at a predetermined setting by first turning on the grinder, then feeding the machine as fast as it will grind. The meal is collected, keeping the loss minimal, the grinder chamber is cleaned, and the fine residue is added to the meal, which is mixed and blended thoroughly. Meal (15 g.) is weighed on a round 20-cm 425-micrometer-opening metal screen over a pan and sifted for 30 sec. on a rotary sifter (190 rpm, 10 cm throw). The assembly is then tapped lightly, and the thrus are weighed. PSI is calculated as the percent of meal passing through the screen. Moisture content of grain is determined by using the Motomco or another official procedure. The grinder is calibrated by determining the PSI of three wheats (a hard red winter, a red soft winter, and a soft white winter wheat) of known PSI by the above procedure. The sum of the indexes should fall within prescribed limits; otherwise, the grinder setting should be adjusted.

In spite of apparent visual differences in vitreosity among grain of a given cultivar attributable to differences in protein content, extensive tests indicate no significant relationship between protein content and PSI within a cultivar (29). The varietal nature of kernel hardness is thus futher confirmed.

PSI for soft wheat is significantly associated with break flour yield obtained in milling the wheat, provided the PSI grinding was done in an appropriate manner (29). This association could be improved if PSI values were adjusted to a uniform moisture content and the millings were done at a given temper moisture.

PSI data may be influenced by grain moisture content, and measurements should be made at similar grain moisture content or the data should be adjusted to a uniform moisture basis to obtain comparable results.

3.4.2 Grinding Resistance Test

A micro hammer mill fitted with a variable speed control and sizing grid was investigated to determine its suitability for measuring grain hardness (30). To determine the optimum load/speed ratio for this a sample of soft English wheat and hard CWRS-1 were tested. Wheat (10, 20, 30 g. respectively) was fed into the mill at various settings and the time required to clear the mill was measured. A sizing grid containing circular holes of 2mm diameter was used. The results indicated that a high load/speed ratio resulted in a marked divergence of clearing times for the hard and soft wheats. Where these times are varying greatly for minor speed differences, large errors could be introduced into the estimation. Also at lower speeds the mill did not run evenly. So a load of 20 g. wheat at a speed setting of 6,100 rpm was used and this provided a good separation between the hard and soft wheats.

Obtaining only a measure of the time to clear the mill would be expected to result in a large dependence on moisture content and this was in fact found to be the case. With both the soft and hard wheats a marked increase in clearing time was noted, although the values obtained remained relative up to a moisture content of 18%. Thus the hardness could be determined at this stage but only in conjunction with an accurate moisture measurement.

To lower the dependence on moisture content and to further accentuate the difference between hard and soft wheats, a measurement of packing density of the meal was incorporated into the determination. This was achieved simply by calibrating tubes, which fitted the mill exit, to a volume of 17 ml. Grinding resistance was then determined as the time taken for the base level of the ground material to reach the calibration mark under the conditions outlined above.

3.4.3 Pearlograph Method

A new method (31) for measuring wheat hardness was developed by modifying a Strong-Scott barley pearler (19). The method involves measuring the torque on the pearler shaft by recording torque versus time plots (pearlograph curves). The physical meaning of the quantities derived from the pearlograph curves are:

1. The best measure of wheat hardness, from the pearlograph, is the chart area beneath the pearlograph torque-time curve. The pearlograph chart height (torque magnitude), at an instant during the pearling process, indicates the material remaining in the pearler.
2. By optimizing the pearling time, the compensating characteristics of the pearlograph curve minimizes the effects of kernel size and distribution.
3. The pearlograph chart area is affected by grain moisture so that, as grain moisture is increased, in the range of 7 to 15 per cent, the chart area for hard wheats decreases rapidly and increases slightly for soft wheat; the areas for the intermediate-hardness wheats are relatively insensitive.
4. The optimum pearling time for which the pearlograph chart area was integrated and used for rating wheat hardness was about 80 sec, on the basis of the maximum ratio of the average effect of variety to that of grain moisture.

3.4.4 Brabender Hardness Tester

Two different models of the Brabender Hardness Tester namely a one-step and a two-step can be used for kernel hardness measurements (32). In the two-step tester, the first burr mill is used to produce a cracked grain product of fairly uniform particle size for the measuring (second) grinder, which is connected to a farinograph torque measuring and recording device. The levers are set as for the 50-g dough mixing bowl. The damper is set to allow the pen to come down from 1,000 to 100 BU in 4 sec, and the chart paper is run at a constant speed of 3.3 cm/min.With two-step tester, varying the gap between the grinding surfaces is not possible. In the one-step BHT, the grinder is connected to the farinograph dynamometer with the levers set as for the 300-g dough mixing bowl. The speed of the chart paper is 40cm/min. The damper is set to allow the pen to come down from 1,000 to 100 BU in 1.5 sec.

3.4.5 Brabender Quadrumat Junior Mill

Twenty grams of wheat were milled on a Brabender Quadrumat Junior Mill, and the product obtained was sieved for 7 min. on an Endecott laboratory sieve shaker with 125-micrometer sieve openings. Two particle size indices were determined from the results (32):

(1) the percentage of the total sample of wheat, in grams, passing through a 125-micrometer sieve (PSI_w) and

(2) the amount of product passing through the 125-micrometer sieve divided by the amount of flour obtained with the same mill for the same size sample (20-g) multiplied by 100 (PSI_f,%).

3.4.5 Comparison of Testing Methods

Comparison of a number of methods of wheat hardness evaluation showed that the WHI and flour yield obtained on the two-step BHT and the WHI from the one-step BHT provide a rapid and sensitive measure of physicomechanical properties of wheat related to hardness. On the basis of these results, the cultivars were properly grouped in wheat class of known hardness. Several other methods ranked wheat classes in the proper order, but these indices were either less sensitive or more time-consuming. PRI did not rank the wheat classes in the same order as the other methods investigated. This discrepancy is presumed to be the result of differences in bran properties. Results of some of the methods investigated were strongly affected by moisture content: they gave the best discrimination at a characteristic "optimum" moisture content.

Numerous other tests for hardness have been used including a measure of resistance to abrasion, of resistance to grinding, of flour released from a single grind and of the resistance of individual grains to crushing or penetration by a stylus. Visual assessment based on the vitreousness of wheats has also been used, but this latter test is most unreliable since the vitreousness of a wheat can be influenced by protein content, degree of weathering and by variety and it is not necessarily related to the actual physical hardness of the wheat.

Tests involving individual kernels have not been very satisfactory due primarily to difficulties in sampling, and several hundred kernels should probably be tested to obtain a meaningful distribution of hardness. In spite of considerable research efforts, a satisfactory hardness measurement for single kernels has not yet been developed.

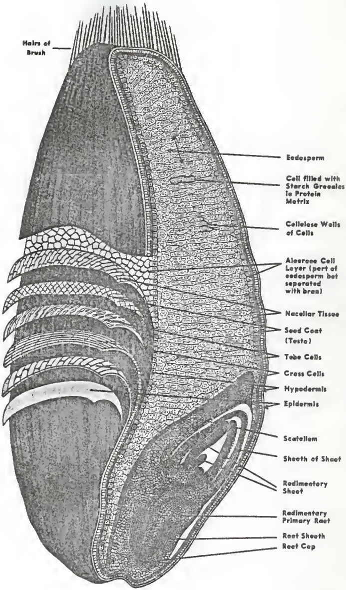

FIG. I LONGITUDINAL SECTION OF GRAIN OF WHEAT

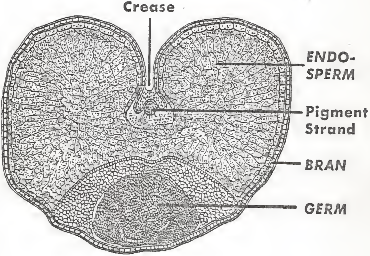

FIG. 2 CROSS SECTION VIEW

CHAPTER IV

KERNEL STRUCTURE AND MICROSCOPIC STUDY

A wheat kernel is often refered to as the one-seeded fruit or, botonically, the caryopsis of the common wheat plant, **Triticum aestivum**. Kernel composition varies more widely in wheat than in any other cereal grain. Although the usual range for protein is from 8 to 15%, values as low as 7% and as high as 24% occur. Genetic differences and cultural conditions, such as temperature, rainfall, cultivation, and soil characteristics, are mainly responsible for compositional variation.

4.1 Kernel Strucuture

The anatomical structure of mature hard red winter wheat was extensively studied by Bradbury et al. (33,34,35,36), and the total microscopic studies of the grain were reviewed by MacMasters et al. (37). The principal parts of the grain, by weight, are the pericarp (5-8%), aleurone layer (6-7%), endosperm (81-83%), embryo (1-1.5%), and scutellum (1.5-2%). These are shown in fig. 1. Surrounding the kernel is pericarp, which can be subdivided into the the epidermis and the inner pericarp, or endocarp. Beneath the pericarp tissue is the seed coat or testa and a hyaline layer, which unites the testa with the aleurone layer. The hyaline layer, so called because it appears bright when seen through a microscope, is also called the nucellar epidermis; it joins a band of cells in the crease referred to as the nucellar projection (Figs. 1 and 2). This band lies just anterior to a pigment strand that in red wheats contains dark-colored pigments. The pigment strand and the nucellar projection run parallel to the length of the crease. The aleurone layer is one cell in thickness and, morphologically, is the outermost part of the endosperm. During milling, the outer coats are removed along with the aleurone layer to give a fraction called bran.

The endosperm, including the aleurone tissue, is responsible for nearly 90% of the total weight of the kernel. Inside the aleurone layer, the endosperm consists of cells tightly packed with starch granules embedded in a protein matrix. Its structure is not homogeneous, but varies depending upon location. The cells underlying the aleurone layer are small and cubical in shape while those closer to the center are larger and polygonal. The outer part of the endosperm is usually vitreous or translucent, often called horny or flinty, and the inner part is opaque, also referred to as floury or mealy. The cells of the subaleurone endosperm layer of U.S. hard red winter wheat (13.7% protein) had protein contents of about 50%; inner endosperm cells of the same wheat had protein contents of about 8% (38).

Endosperm texture is one of the most constant characteristics associated with different classes and varieties. Typically, durum or macaroni wheat is hard and has translucent endosperm. Soft red winter wheats generally have a soft or floury endosperm. Hard red wheats have either a hard endosperm or a combination of vitreous and soft endosperm. In endosperms having both textures the floury part is usually located near the embryo, while the apical portion is horny.

The germ or embryo is composed of two major parts- the embryonic axis, which during germination develops into the seedling, and the scutellum, which provides nutrients to the seedling. The embryonic axis is composed of the shoot (plumule) and the primary root. Coleoptile is a protective sheath covering the plumule, and the coleorhiza covers the primary root. Besides the primary root, two pairs of secondary rootlets have been formed. Attached to the side of the embryonic axis nearest the endosperm is the scutellum of the embryo.

4.2 Electron Microscopic Studies of the Kernel Structure

A. General

Even though both types of hard and soft wheats contain the same two major building materials, protein and starch something causes hard wheats to be harder than soft wheats. Three possible explanations can be given:

(1) variation in the ratio of protein to starch
(2) starch and protein components are intrinsically harder in hard wheats, and
(3) binding forces between starch and protein differ.

The ratio of starch to protein content varies in wheats, but experimental evidence indicates that this variation is not responsible for the observed differences in hardness (39). A soft wheat variety grown under conditions designed to produce higher than normal protein content will still be relatively soft. Conversely, a low protein hard wheat variety will still be relatively hard.

Inherent differences in the protein or starch components of hard and soft wheat are also apparently inadequate to explain differences in kernel hardness. In spite of the different end-uses of hard and soft wheat flours, it appears that the difference is the quantitative rather than the qualitative variation between the fractions. Although, both types of wheats vary genetically, particularly in the protein fraction, the amount and the quality of the protein overlap (39). Convincing evidence that the difference in hardness was not due to intrinsic hardness differences in components was provided by Barlow and Simmonds (40). Those authors and Wrigley (41,42) attribute the differences in hardness to variations in the adhesion between the starch and protein components. In order to visualize the structural differences between hard and soft wheats electron micrographs have been taken using a Hitachi HU-11 B Transmission Electron Microscope (TEM). The preparation of the wheat samples for the TEM studies are described below.

B. Sample Preparation

The wheat samples were cut into small pieces approximately of the order of 1 cm^3. To these small pieces, 6% Glutaraldehyde was added and the buffer PIPES (0.08 molar, PH=8) was used and fixed at room temperature for 4 hours. Then they were washed in 0.18 molar, PH = 6.8 buffer PIPES for 1.5 hours and then fixed with Osmium tetroxide at 2% in 0.18 molar PIPES for 2 hours. The samples were dehydrated in alcohol and then infiltrated with Spurr's embedding plastic. The samples were sectioned after 48 hours of curing at 70 $^{\circ}$ C. Sections were collected on grids and then stained with 1% Uranyl acetate and Renold's lead citrate in order to have a good contrast when viewed through the microscope.

C. TEM Micrographs and Analysis

The TEM wheat samples were viewed at an accelerating voltage of 75 K eV, using pole piece # 3. A micrographic cross-section of the soft wheat has been shown in Fig.3, having a magnification factor of 3750 X whereas figures 4 and 5 show the micrographic cross-section of hard wheat with magnification equal to 3000 X. The lens system currents have been tabulated in Table 1.

The magnification for each micrograph has been determined from the standard calibration curve of intermediate lens current versus magnification under constant conditions of accelerating voltage (V_o = 75 KeV, I_o = 115 to 117 mA, I_p = 110 mA, and using pole piece # 3). Figures 1, 4, and 5 give an overall idea about the cross sectional view of the wheat samples. In these pictures, the starch cells embedded in protein matrix have been marked. Figures 2 and 6 show a single starch cell embedded in the protein matrix. These pictures respectively correspond to the soft and hard wheat samples and have been taken in order to view more clearly what happens in an isolated cell. Finally, selected area diffraction pictures (SAD) have been taken of isolated cells by introducing an objective aperture in the back focal plane of the objective (Figures 3 and 7). These pictures help to determine the degree of crystallinity of the wheat samples.

Comparison of TEM pictures clearly shows that there exist structural differences between hard and soft wheat samples. In particular, the voids (V) in between the starch cells (S) and the protein matrix (P) of the hard

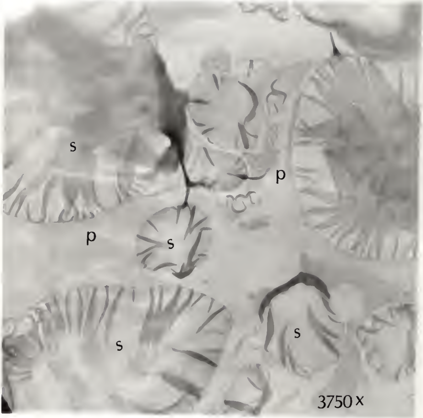

FIG. 3 A CROSS SECTION OF SOFT WHEAT

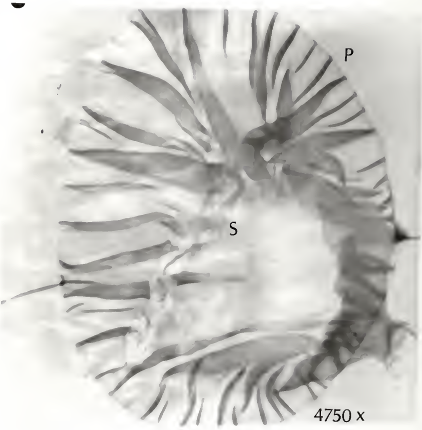

FIG. 4 A TEM PICTURE OF SINGLE STARCH CELL EMBEDDED IN PROTEIN MATRIX OF A SOFT WHEAT

FIG. 5 SAD OF SINGLE STARCH CELL OF A SOFT WHEAT

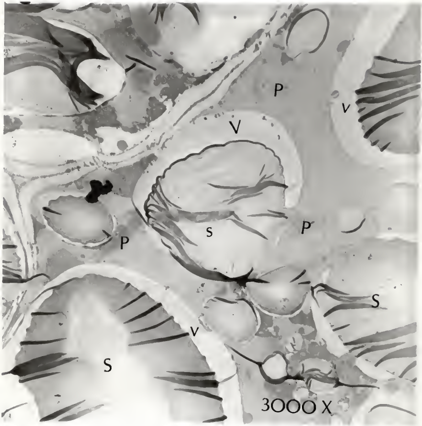

FIG. 6 A CROSS SECTION OF HARD WHEAT SAMPLE FROM TEM

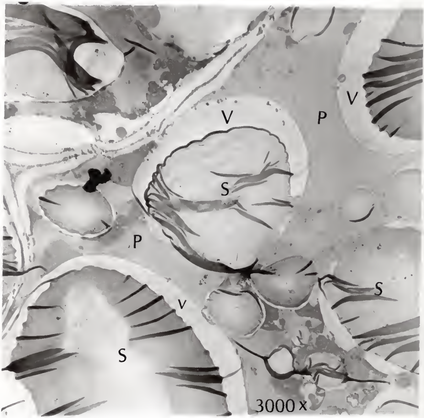

FIG. 7 A CROSS SECTION OF HARD WHEAT SAMPLE FORM TEM

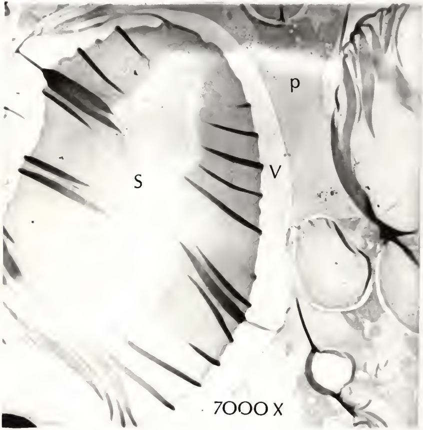

FIG. 8 A TEM PICTURE OF SINGLE STARCH CELL EMBEDDED IN PROTEIN MATRIX OF A HARD WHEAT

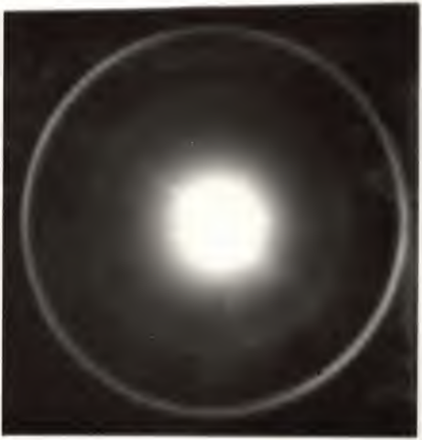

FIG. 9 SAD OF SINGLE STARCH CELL OF A HARD WHEAT

wheat indicate that the air spaces probably are formed after physiological maturity during the drying of the kernel. But in the soft wheat samples, there are no such voids supporting the idea of the expected structural differences between the two varieties. As the wheat loses water, the protein shrinks, ruptures and leaves air spaces. In harder wheat, the kernel becomes denser during drying but the protein matrix remains intact. TEM of wheats suggests that hardness of wheat is determined by the strength of the protein-starch bond. This conclusion agrees with Wrigley's (42) postulate which was based on chemical work.

TABLE 1. LENS SYSTEM CURRENTS

Accelerating Voltage = 75 KeV; Pole piece # : 3

Fig. #	I_{c1} mA	I_{c2} mA	I_o mA	I_I mA	I_p mA	mag. X
1	67	48	117	42	109	3750
2	67	47	117	44	111	4750
3	67	44.5	119	47	111	6000
4	78	52	114	40	107.5	3000
5	78	52	114	40	107.5	3000
6	78	54	113	49	107	7000
7	78	57.5	120	49	107.5	7000

I_{c1} - First condenser lens current.
I_{c2} - Second condenser lens current.
I_o - Objective lens current.
I_I - Intermediate lens current.
I_p - Projection lens current.

When both the wheat samples were tested for their crystalline nature by using SAD technique, a central bright spot surrounded by a diffused ring pattern was obtained for the soft wheat sample, which clearly reveals the amorphous nature of the soft wheat. But in the case of hard wheat sample, the central bright spot is surrounded by a sharp ring indicating that the hard wheat is more crystalline in nature. In order to have a good contrast, Uranyl acetate and REYNOLD's lead citrate were used in the sample preparation and this might lead to a sharp ring coming from the lead content in the samples. Considering this fact it is possible that both varieties of wheat are amorphous in nature.

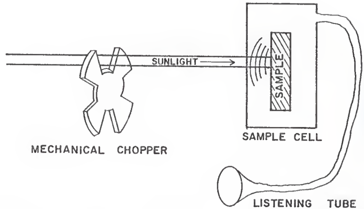

FIG.10 ILLUSTRATION OF PHOTOACOUSTIC EFFECT

CHAPTER V

THEORY OF PHOTOACOUSTIC EFFECT OF SOLIDS

5.1 Introduction

In its broadest sense, spectroscopy can be defined as the study of the interaction of energy with matter. As such, it is a science encompassing many disciplines and many techniques. In the field of high-energy physios, the radiation is sufficiently energetic to seriously perturb, and in some cases, even transform the matter with which it interacts. On the other hand, in the oldest form of spectroscopy, optical spectroscopy, the enegy is usually too low to perturb or noticeably alter the material under study. The energy used in optical spectroscopy exists in the form of optical photons or quanta, with wavelengths ranging from less than 100 nm in the vacuum ultraviolet, to more than 100 microns in the far-infrared. Because of its versatality, range, and nondestructive nature, optical spectroscopy remains a widely used and most important tool for investigating and characterizing the properties of matter.

The two most common techniques in the optical region are absorption and reflection spectroscopy. Many organic and inorganic materials, such as powders, amorphous compounds, smears, gels and oils, can not be readily studied by either of these two techniques. Methods involving diffuse or attenuated total reflectance permit the study of some of these materials but they possess severe drawbacks.

During the past few years, another optical technique has been developed to study those materials that are unsuitable for the conventional transmission or reflection methodologies (43, 44, 45). This technique, called photoacoustic spectroscopy or PAS, is different than the conventional techniques chiefly in that even though the incident energy is in the form of optical photons, the interaction of these photons with the material under investigation is studied not through subsequent detection and analysis of some of the photons, but rather through a direct measure of the energy absorbed by the material as a result of its interaction with the photon beam.

The photoacoustic effect is the process of generating an acoustic wave by the absorption of an amplitude-modulated light beam. The process was invented in 1880 by Bell, Tyndall and Roentgen. In early experiments, sunlight was focused onto a sample in a cell that was connected to a listening tube and this earlier experimental set-up is illustrated in Fig. 10. When the beam of sunlight was periodically interrupted by a chopping wheel, sound could be heard through the listening tube at the sunlight chopping frequency. Bell noted that, "the loudest signals are produced from substances in a loose, porous, spongy condition, and from those that have the darkest or most absorbent colors" (46). The effect was ignored until 1968, when it was revived by Rosencwaig and others at Bell Laboratories. The availability of powerful light sources, such as lasers, transformed a laboratory curiosity into a powerful analytical tool.

In modern studies utilizing the photoacoustic effect the sample to be studied is usually placed in a closed cell. For solids the sample usually occupies only part of the cell, the remainder of the volume being filled with a nonabsorbing gas. The sample chamber also contains a sensitive microphone. A modulated light beam is allowed to strike the sample and surface of the sample is periodically heated as light is absorbed and cooled as the light is interrupted. Heat from the sample surface diffuses into the gas in the cell to produce a boundary layer of gas, directly adjacent to the surface, whose temperature varies at the modulation frequency. The heating and cooling of the gas layer produces an acoustic wave in the gas which is detected by the microphone. In obtaining a photoacoustic spectrum, one records the microphone signal as a function of the wavelength of light incident on the sample. Since the strength of the acoustic signal is proportional to the amount of light absorbed by the sample, there is a close correspondence between a photoacoustic spectrum and a conventional optical absorption spectrum. Furthermore, since only absorbed light can produce an acoustic signal, scattered light, which often presents a serious problem in conventional spectroscopy, presents no serious problem in PAS.

There are several advantages to photoacoustics as a form of spectroscopy. Since absorption of optical or electromagnetic radiation is required before a photoacoustic signal can be generated, light that is transmitted or elastically scattered by the sample is not detected and hence does not interfere with the inherently absorptive PAS measurements. This is of crucial importance when one is working with essentially transparent media, such as pollutant- containing gases, that have few absorbing centers. The insensitivity to scattered radiation also permits the investigator to obtain optical absorption data on highly light-scattering materials, such as powders, amorphous solids, gels, and colloids. Another advantage is the capability of obtaining optical absorption spectra on materials that are completely opaque to transmitted light since the technique does not depend on the detection of photons. Coupled with this is the capability, unique to PAS, of performing nondestructive depth-profile analysis of absorption as a function of depth into an opaque material. Finally, the photoacoustic effect results from a radiationless energy-conversion process and is therefore complemen-

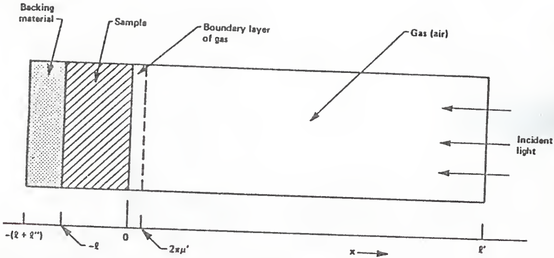

FIG. II CROSS SECTIONAL VIEW OF A SIMPLE CYLINDRICAL PHOTOACOUSTIC CELL.

tary to radiative and photochemical processes. Thus PAS itself may be used as a sensitve, though indirect, method for studying the phenomena of flourescence and photosensitivity in matter.

The next session 5.2 has been devoted to the fundamental theoretical aspects of PAS of solids, before proceeding to the experimental set-up and further details.

5.2 Rosencwaig-Gersho Theory

5.2.1 The Thermal Diffusion Equations

Any light absorbed by the solid is converted, in part or in whole, into heat by non-radiative deexcitation processes within the solid. To start with let us consider the Rosencwaig-Gersho theory, a one-dimensional analysis of the production of a photoacoustic signal in a simple cylindrical cell such as the one depicted in Figure 11. The photoacoustic cell has a diameter D and length L. We assume that the length L is small compared to the wavelength of the acoustic signal, and the microphone (not shown) detects the average pressure produced in the cell. The sample is considered to be in the form of a disc having diameter D and thickness l. The sample is mounted so that its back surface is against a poor thermal conductor of thickness l". The length l" of the gas column in the cell is then given by l" = L-l-l'. We further assume that the gas and backing materials are not light absorbing.

We define the following parameters:

k: thermal conductivity (cal/cm-sec-^{o}C)
p: density (g/cm^3)
C: specific heat (cal/g-^{o}C)
$\alpha = k/\rho C$: thermal diffusivity (cm^2/sec)
$a = (\omega/2\alpha)^{1/2}$: thermal diffusion coefficient (cm^{-1})
$\mu = 1/a$: thermal diffusion length (cm)

where ω denotes the chopping frequency of the incident light beam in radians per second. In the following treatment, we denote sample parameters by unprimed symbols, gas parameters by singly primed symbols, and backing material parameters by doubly primed symbols.

We assume a sinusoidally chopped monochromatic light source with wavelength λ incident on the solid with intensity

$$I = \tfrac{1}{2} I_0 (1+\cos\omega t) \qquad (1)$$

where I_0 is the monochromatic light flux (W/cm^2). We let β denote the optical absorption coefficient of the solid sample (in reciprocal centimeters) for the wavelength λ. The heat density produced at any point due to light absorbed at this point in the solid is then given by

$$\tfrac{1}{2}\beta I_0 e^{\beta x}(1+\cos\omega t) \qquad (2)$$

where x takes on negative values since the solid extends from x=0 to x=-l, with the light incident at x=0. Note also from Figure 11 that the air column extends from x=0 to x=l' and the backing from x=-l to x=-(l+l").

The thermal diffusion equation in the solid taking into account the distributed heat source can be written as

$$\frac{\partial^2\theta}{\partial x^2} = \frac{1}{\alpha}\frac{\partial\theta}{\partial t} - Ae^{\beta x}(1+e^{i\omega t}) \quad \text{for } -l < x < 0 \qquad (3)$$

with

$$A = \frac{\beta I_0 \eta}{2\kappa} \qquad (4)$$

where θ is the temperature and η is the efficiency at which the abosorbed light at wavelength λ is converted to heat by the nonradiative deexcitation processes. We assume $\eta = 1$, a reasonable assumption for most solids at room temperature. For the backing and the gas, the heat diffusion equations are respectively given by

$$\frac{\partial^2\theta}{\partial x^2} = \frac{1}{\alpha''}\frac{\partial\theta}{\partial t} \quad -l'' - l < x < -l \qquad (5)$$

$$\frac{\partial^2\theta}{\partial x^2} = \frac{1}{\alpha'}\frac{\partial\theta}{\partial t} \quad 0 < x < l' \qquad (6)$$

The real part of the complex valued solution $\theta(x,t)$ of (3)-(6) is the solution of physical interest and represents the temperature in the cell relative to ambient temperature as a function of position and time. Thus the actual temperature field in the cell is given by

$$T(x,t) = \mathrm{Re}\,\theta(x,t) + \phi_0 \qquad (7)$$

where Re denotes the "real part of" and ϕ_0 is the ambient (room) temperature.

To completely specify the solution of (3), (5), and (6) the appropriate boundary conditions are obtained from the requirement of temperature and heat flux continuity at the boundaries x=0 and x=-l, and from the constraint that the temperature at the cell walls x=+l' and x=-l-l" is at ambient. The latter constraint is a reasonable assumption for metallic cell walls, but in any case it does not affect the ultimate solution for the acoustic pressure. Finally, we make the assumption that the dimensions of the cell are small enough to ignore convective heat flow in the gas at steady-state conditions.

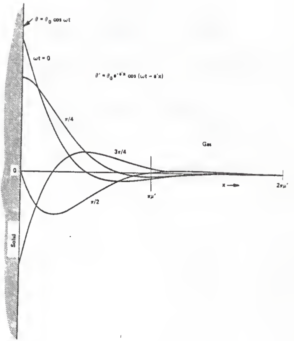

FIG. 12 SPATIAL VARIATION OF THE TIME-DEPENDENT TEMPERATURE AT THE GAS-SAMPLE INTERFACE.

5.2.2 Temperature Distribution in the Cell

The general solution for θ (x, t) in the cell neglecting transients can be written as

$$\theta(x,t) = \begin{cases} \frac{1}{l}(x+l+l")W_0 + We^{\sigma"(x+l)}e^{i\omega t} & -l-l"<x<-l \\ b_1+b_2x+b_3e^{\beta x}+(Ue^{\sigma x}+Ve^{-\sigma x}+-Ee^{\beta x})e^{i\omega t} & -l<x<0 \\ (1-\frac{x}{l'})F+\theta_0 e^{-\sigma' x}e^{i\omega t} & 0<x<l' \end{cases} \quad (8)$$

where W, U, V, E, and θ_0 are complex valued constants b_1, b_2, b_3, W_0, and F are real valued constants, and $\sigma = (1+i)a$ with $a = (\omega/2\alpha)^{1/2}$. In particular it should be noted that θ and W represent the complex amplitudes of the periodic temperatures at the sample-gas boundary (x=0) and the sample-backing boundary (x= -l), respectively. The d.c. solution in the backing and gas already make use of the assumption that the temperature (relative to ambient) is zero at the ends of the cell. The quantities W_0 and F denote the d.c. component of the temperature (relative to ambient) at the sample surfaces x=-l and x=0, respectively. The quantities E and b_3, determined by the forcing function in (3), are given by

$$b_3 = \frac{-A}{\beta^2} \quad (9)$$

$$E = \frac{A}{(\beta^2-\sigma^2)} = \frac{\beta I_0}{2\kappa(\beta^2-\sigma^2)} \quad (10)$$

In the general solution (8) we omit the growing exponential component of the solutions to the gas and backing material because for all frequenccies ω of interest the thermal diffusion length is small compared to the length of the material in both the gas and the backing. That is $\mu" < l"$ and $\mu' \leq l'$, and hence the sinusoidal components of these solutions are sufficiently damped so that they are effectively zero at the cell walls. Therefore, to satisfy the temperature constraint at the cell walls, the growing exponential components of the solutions would have coefficients that are essentially zero. The temperature and flux continuity conditions at the sample surfaces are explicitly given by

$$\theta'(0,t) = \theta(0,t) \quad (11a)$$

$$\theta"(-l,t) = \theta(-l,t) \quad (11b)$$

$$\kappa' \frac{\partial\theta}{\partial x}(0,t) = \kappa\frac{\partial\theta}{\partial x}(0,t) \quad (11c)$$

$$\kappa" \frac{\partial\theta"}{\partial x}(-l,t) = \kappa\frac{\partial\theta}{\partial x}(-l,t) \quad (11d)$$

These constraints apply separately to the d.c. component and the sinusoidal component of the solution. From (11) we obtain for the d.c. components of the solution

$$F_0 = b_1+b_3 \qquad (12a)$$

$$W_0 = b_1-b_2 l+b_3 e^{-\beta l} \qquad (12b)$$

$$\frac{-\kappa'}{l'} F_0 = \kappa b_2+\kappa\beta b_3 \qquad (12c)$$

$$\frac{\kappa''}{l''} W_0 = \kappa b_2+\kappa\beta b_3 e^{-\beta l} \qquad (12d)$$

Equations (12) determine the coefficients b_1, b_2, b_3, W_o, and F_o for the time-independent (d.c.) component of the solution. Applying (11) to the sinusoidal component of the solution yields:

$$\theta_0 = U+V-E \qquad (13a)$$

$$W = e^{-\sigma l}U+e^{\sigma l}V-e^{-\beta l}E \qquad (13b)$$

$$-\kappa'\sigma'\theta_0 = \kappa\sigma U-\kappa\sigma V-\kappa\beta E \qquad (13c)$$

$$\kappa''\sigma''W = \kappa\sigma e^{-\sigma l}U-\kappa\sigma e^{\sigma l}V-\kappa\beta^{-\beta l}E \qquad (13d)$$

These quantities together with the expression for E in (10) determine the coefficients U,V,W, and θ_0. Hence the solutions to (12) and (13) allow us to evaluate the temperature distribution (8) in the cell in terms of the optical, thermal, and geometric parameters of the system. The explicit solution of θ_0, the complex amplitude of the periodic temperature at the solid-gas boundary (x=0) is given by

$$\theta_0 = \frac{\beta I_0}{2\kappa(\beta^2-\sigma^2)} \; \frac{(r-1)(b+1)e^{\sigma l}-(r+1)(b-1)e^{-\sigma l}+2(b-r)e^{-\beta l}}{(g+1)(b+1)e^{\sigma l}-(g-1)(b-1)e^{-\sigma l}} \qquad (14)$$

where $$b = \frac{\kappa''a''}{\kappa a} \qquad (15)$$

$$g = \frac{\kappa'a'}{\kappa a} \qquad (16)$$

$$r = (1-i)\frac{\beta}{2a} \qquad (17)$$

and, as is stated earlier, $\sigma=(1+i)a$. Thus (14) can be evaluated for specific parameter values, yielding a complex number whose real and imaginary parts, θ_0 and θ_2, respectively determine the in-phase and quadrature components of the periodic temperature variation at the surface x=0 for the sample. Specifically, the actual temperature at x=0 is given by

$$T(0,t) = \phi_0+F_0+\theta_1\cos\omega t-\theta_2\sin\omega t \qquad (18)$$

where ϕ_0 is the ambient temperature at the cell walls and F_o is the increase in temperature due to the steady-state component of the absorbed heat.

5.2.3 Production of the Acoustic Signal

As is stated at the beginning of this chapter, it is our contention that the main source of the acoustic signal arises from the periodic heat flow from the solid to the surrounding gas. The periodic diffusion process produces a periodic temperature variation in the gas as given by the sinusoidal (a.c) component of the solution (8),

$$\theta_{a.c.}(x,t) = \theta_0 e^{-\sigma' x} e^{i\omega t} \tag{19}$$

Taking the real part of (19), we see that the actual physical temperature variation in the gas is

$$T_{a.c.}(x,t) = e^{-a'x}[\theta_1 \cos(\omega t - a'x) - \theta_2 \sin(\omega t - a'x)] \tag{20}$$

where θ_1 and θ_2 are the real and imaginary parts of θ_0, as given by (14). As can be seen in Figure 12, the time-dependent component of the temperature in the gas attenuates rapidly to zero with increasing distance from the surface of the solid. At a distance of only $2\pi/a' = 2\pi\mu'$, where μ' is the thermal diffusion length in the gas, the periodic temperature variation in the gas is effectively fully damped out. Thus we can define a boundary layer, as shown in Figure 11, whose thickness is $2\pi\mu'$ (≈ 0.1 cm at $\omega/2\pi \approx 100$ Hz) and maintain to a good approximation that only this thickness of gas is capable of responding thermally to the periodic temperature at the surface of the sample.

The spatially averaged temperature of the gas within this boundary layer as a function of time can be determined by evaluating

$$\bar{\theta}(t) = \frac{1}{2\pi\mu'} \int_0^{2\pi\mu} \theta_{a.c.}(x,t)dx \tag{21}$$

From (19)

$$\bar{\theta}(t) \simeq \frac{1}{2\sqrt{2\pi}} \theta_0 e^{i(\omega t - \pi/4)} \tag{22}$$

using the approximation $e^{-2\pi} \ll 1$.

Because of the periodic heating of the boundary layer, this layer of gas expands and contracts periodically and thus can be thought of as acting as an acoustic piston on the rest of the gas column, producing an acoustic pressure signal that travels through the entire gas column. A similar argument has been used successfully to account for the acoustic signal produced when a conductor in the form of a thin flat sheet is periodically heated by an a.c. electrical current.

The displacement of this gas piston due to periodic heating can be estimated by using the ideal gas law,

$$\delta x(t) = 2\pi\mu'\frac{\bar{\theta}(t)}{T_0} = \frac{\theta_0\mu'}{\sqrt{2}\,T_0}e^{i(\omega t-\pi/4)} \tag{23}$$

where we have set the average d.c. temperature of this gas boundary layer equal to the d.c. tempearature at the solid surface, $T_0 = \phi_0 + F_0$. Equation (23) is a reasonable approximation to the actual displacement of the layer since $2\pi\mu'$ is only ~ 0.1 cm for $\omega/2\pi = 100$ Hz and even smaller at higher frequencies.

If we assume that the rest of the gas responds to the action of this piston adiabatically, then the acoustic pressure in the cell due to the displacement of this gas piston from the adiabatic gas law

$$PV^{\gamma} = \text{constant} \tag{24}$$

where P is the pressure, V is the volume in the cell, and is the ratio of the specific heats. Thus the incremental pressure is

$$\delta P(t) = \frac{\gamma P_0}{V_0}\,\delta V = \frac{\gamma P_0}{l'}\,\delta x(t) \tag{25}$$

where P_0 and V_0 are the ambient pressure and volume, respectively, and $-\phi V$ is the incremental volume. Then from (23),

$$\phi P(t) = Qe^{i(\omega t-\pi/4)} \tag{26}$$

where

$$Q = \frac{\gamma P_0\theta}{\sqrt{2}\,l'a'T_0} \tag{27}$$

Thus the actual physical pressure variation, $\Delta p(t)$, is given by the real part of $\delta P(t)$ as

$$\Delta p(t) = Q_1\cos(\omega t-\tfrac{\pi}{4}) - Q_2\sin(\omega t-\tfrac{\pi}{4}) \tag{28}$$

or

$$\Delta p(t) = q\cos\,(\omega t-\psi-\tfrac{\pi}{4}) \tag{29}$$

where Q_1 and Q_2 are the real and imaginary parts of Q, and q and $-\psi$ are the magnitude and phase of Q, that is,

$$Q = Q_1 + iQ_2 = qe^{-i\psi} \tag{30}$$

Thus Q specifies the complex envelope of the sinusoidal pressure variation. Combining (14) and (27) we get the explicit the formula

$$Q = \frac{\beta I_0\gamma P_0}{2\sqrt{2}\,T_0\kappa l'a'(\beta^2-\sigma^2)} \times \frac{(r-1)(b+1)e^{\sigma l}-(r+1)(b-1)e^{-\sigma l}+2(b-4)e^{-\beta l})}{(g+1)(b+1)e^{\sigma l}-(g-1)(b-1)e^{-\sigma l}} \tag{31}$$

where $b = k''a''/ka$, $g = k'a'/ka$, $r = (1-i)\beta/2a$ and $\sigma = (1+i)a$ as is defined earlier. At ordinary temperatures $T_0 \simeq \phi_0$ so that the

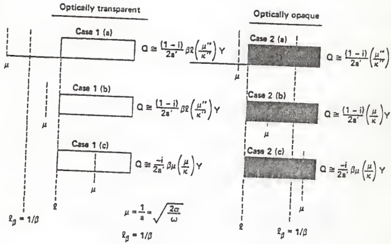

FIG. 13 SCHEMATIC REPRESENTATION OF THE SPECIAL CASES FOR THE PHOTO - ACOUSTIC THEORY OF SOLIDS.

d.c. components of the temperature distribution need not be evaluated. Thus (31) may be evaluated for the magnitude and phase of the acoustic pressure wave produced in the cell by the photoacoustic effect.

5.3 SPECIAL CASES

The full expression for $\Delta p(t)$ is somewhat difficult to interpret because of the complicated expression of Q as given by (31). However, physical insight may be gained by examining special cases where the expression for Q becomes relatively simple. We group these cases according to the optical opaqueness of the solids as determined by the relation of the optical absorption length $l_\beta = 1/_\beta$ to the thickness l of the solid. For each category of optical opaqueness, we then consider three cases according to the relative magnitude of the thermal diffusion length μ, as compared to the physical length l and the optical absorption length l_β. For all the cases evaluated below, we make use of the reasonable assumption that $g < b$ and that $b \sim 1$, this is that $k'a' < k''a''$ and $k''a'' \simeq k''a$.

The six cases are shown in Figure 13. It is convenient to define

$$Y = \frac{\gamma P_0 l_0}{2\sqrt{2}\, T_0 l'}, \tag{32}$$

which always appears in the expression for Q as a constant factor. We also define the optical path length as

$$l\beta = \frac{1}{\beta} \tag{33}$$

5.3.1 Optically Transparent Solids ($l_\beta > l$)

In these cases, the light is absorbed throughout the length of the sample, and some light is transmitted through the sample.

Case 1a: Thermally-Thin Solids ($\mu >> l; \mu > l$)
Here we set $e^{-\beta l} \beta l - \beta l, e^{\pm \sigma l} \simeq 1$, and $|r| > 1$ in (31). We then obtain

$$Q = \frac{Y}{2a'a''\kappa''}(\beta - 2ab - i\beta) \simeq \frac{(1-i)\beta l}{2a'}\left(\frac{\mu''}{\kappa''}\right)Y \tag{34}$$

The acoustio signal is thus proportional to βl, and since μ''/a' is proportional to $1/\omega$, the acoustic signal has an ω^{-1} dependence. For this thermally thin case $\mu >> l$ the thermal properties of the backing material come into play in the expression for Q.

Case 1b: Thermally-Thin solids ($\mu > l$; $\mu < l_\beta$)

Here we set $e^{-\beta l} \simeq 1-\beta l$, $e^{\pm\sigma l}(1\pm\sigma l)$, and $|r| < 1$ in (31).

We then obtain

$$Q = \frac{\beta l Y}{4\kappa a' a^3 b}[(\beta^2+2a^2)+i(\beta^2-2a^2)] \simeq \frac{(1-i)\ l}{2a}\left(\frac{\mu''}{\kappa''}\right) Y \qquad (35)$$

The acoustic signal is again proportional to βl, varies as ω^{-1} and depends on the thermal properties of the backing material. Equation (35) is identical to (34).

Case 1c: Thermally-Thick Solids ($\mu > l$; $\mu << l_\beta$)

In (31) we set $e^{-\beta} \simeq 1-\beta l$, $e^{-\sigma l} \simeq 0$, and $|r| << 1$. The acoustic signal then becomes

$$Q \simeq -i\frac{\beta\mu}{2a'}\left(\frac{\mu}{\kappa}\right) Y \qquad (36)$$

Here the signal is proportional to $\beta\mu$ rather than βl diffusion length contributes to the signal, in spite of the fact that light is being absorbed throughout the length l of the solid. Also since $\mu < l$, the thermal properties of the backing material present in (35) are replaced by those of the sample. The frequency dependence of Q in (36) varies as $\omega^{-3/2}$.

Cases 1a, 1b, and 1c for the so-called optically transparent demonstrate a unique capability of photoacoustic spectroscopy, to wit, the capability of obtaining a depth profile of optical absorption within a sample; that is, by starting at a high chopping frequency we can obtain optical absorption information from only a layer of material near the surface of the solid. For materials with low thermal diffusivity this layer can be as small as 0.1 µm at chopping frequencies of 10,000-100,000 Hz. Then by decreasing the chopping frequency, we increase the thermal diffusion length and optical absorption data further within the material, until at ~5Hz we can obtain data down to 10-100 µm for materials with low thermal diffusivities and upto 1-10 mm for materials with high thermal diffusivities. This capability for depth-profile analysis is unique and opens up exciting possibilities in studying layered and amorphous materials and in determining overlay and thin film thickness.

5.3.2 <u>Optically Opaque Solids</u> ($l_\beta << l$)

In these cases, most of the light is absorbed within a distance that is small compared to l, and essentially no light is transmitted.

Case 2a: Thermally-Thin Solids ($\mu >> l$; $\mu >> l_\beta$)

In (31), we set $e^{-\beta l} 0, e^{\pm \sigma l} \approx 1$, and $|r| >> 1$. We then obtain

$$Q \approx \frac{(1-i)}{2a} \left(\frac{\mu''}{\kappa''}\right) Y \quad (37)$$

In this case, we have photoacoustic "opaqueness" as well as optical opqueness, in the sense that our acoustic signal is independent of β. This would be the case for a very black absorber such as carbon black. The signal is quite strong (it is $1/\beta l$ times as strong as that in case 1a), depends on the thermal properties of the backing material, and varies as ω^{-1}.

Case 2b: Thermally-Thick Solids ($\mu < l$; $\mu > l_\beta$)

In (31) we set $e^{-\beta l} \approx 0$, $e^{-\sigma l} \approx 0$, and $|r| > 1$. We obtain

$$Q \approx \frac{Y}{2a'a\kappa\beta} (\beta - 2a - i\beta) \approx \frac{(1-i)}{2a'} \left(\frac{\mu}{\kappa}\right) Y \quad (38)$$

Equation (37) is analogous to (37), but the thermal parameters of the backing are now replaced by those of the solid. Again the acoustic signal is independent of β and varies as ω^{-1}.

Case 2c: Thermally-Thick Solids ($\mu << l$; $\mu > l_\beta$)

We set $e^{-\sigma l} \approx 0$, $e^{-\sigma l} \approx 0$, and $|r| < 1$ in (31). We obtain

$$Q = \frac{-i\beta Y}{4a'a^3\kappa}(2a - \beta + i\beta) \approx \frac{-\beta\mu}{2a'}\left(\frac{\mu}{\kappa}\right) Y \quad (39)$$

This is a very interesting and important case. Optically we are dealing with a very opaque solid ($\beta l >> 1$). However, as long as $\beta\mu < 1$ (i.e., $\mu < l_\beta$) this solid is not photoacoustically opaque, since, as in case 1c, only the light absorbed within the first thermal diffusion length, μ, contributes to the acoustic signal. Thus even though this solid is optically opaque, the photoacoustic signal is proportional to β. As in 1c, the signal is also dependent on the thermal properties of the sample and varies as $\omega^{-3/2}$.

5.4 Summary

Theoretical formulas show that the photoacoustic signal is ultimately governed by the magnitude of the thermal diffusion length of the solid. Thus even when a solid is optically opaque, it is not necessarily opaque photoacoustically and, in fact, as long as $\beta\mu < 1$, the photoacoustic signal will be proportionalt to β even though the optical thickness βl of the sample may be much greater than unity. Since the thermal diffusion length μ_s can be changed by changing the chopping frequency ω, it is therefore possible, with the photoacoustic technique, to obtain optical absorption spectra on any, but the most highly opaque, solids. This capability of the PAS technique together with its insensitivity to scattered light makes its use as a spectroscopic tool for the investigation of solid and semisolid materials highly attractive.

With its various spectroscopic and nonspectroscopic attributes, photoacoustics has already found many important applications in the research and characterization of materials. Photoacoustic studies are performed on all types of materials, inorganic, organic, and biological, and on all three matter states - gas, liquid, and solid.

CHAPTER VI

DESCRIPTION OF PHOTOACOUSTIC APPARATUS

It is said that history has a habit of repeating itself, and this trend can certainly be seen as we look back through the story of research in any field. So often it seems that much the same experiment has been performed on different occasions. The aim has been similar each time; but newer techniques have been focused on the problem on each occasion, so new knowledge has been won with each cycle. Much in the same way, even though many techniques are available in differentiating the hard and soft wheats, a new technique based on the principle of photoacoustics has been tried in this thesis work in order to have further improvement in characterization of wheat kernels.

6.1 General Criteria for a Photoacoustic Set-Up

A photoacoustic experiment is composed of three main parts: a source of incoming radiation, the experimental chamber, and the data acquisition system.

A. Radiation Sources

A common and most economical source of optical radiation in the ultraviolet, visible, and infrared regions is provided by conventional light generators in conjunction with a monochromator. These light sources are the arc lamp for the uv-visible, the incandescent lamp for the visible and near infrared, and the glow bar for the mid-to-far infrared regions. Since all three light sources provide a broadband optical radiation, they must be used in conjunction with suitable monochromators. It is known that the signal-to-noise ratio of the photoacoustic response increases linearly with the light intensity impinging on the sample (47). Thus, it is advantageous to use an intense light source and a high light throughput (i.e., low f number) monochromator. Since the conventional light sources operate in a continuous mode, a light chopper, usually electromechanical in nature, must be used. This chopper can be located before or after the monochromator. In the theory of the photoacoustic effect in solids (47, 48), it has been shown that the optical absorption spectra of completly opaque samples can be obtained, and that absorption versus depth studies can be performed, provided one is able to adjust the chopping frequency. Thus for optimum versatility, a variable speed chopper is to be recommended. Another source of optical radiation which can be used in photoacoustic experiments is the laser. A laser requires no monochromator and if operated in a pulsed mode would also require no chopper. For example, in the visible wavelength region, dye lasers provide an intense highly monochromatic light readily tunable over a fairly large wavelength range.

For the present study, since we were not attempting to measure photoacoustic absorption spectra, we chose to use light-emitting diodes sources. These are cheap, powerful light sources that are easily modulated and that produce radiation bands from green to near infrared, depending on the diode selected.

B. Experimental Chamber

The experimental chamber contains the photoacoustic cell and all the required optics. The actual design of this chamber will vary depending on whether one is using a single beam system employing only one photoacoustic cell, or a double beam-system containg two cells, with appropriate beamsplitting optics. The photoacoustic cell will generally incorporate a suitable microphone with its pre-amplifier. Both a conventional condenser microphone with external biasing, and an electret microphone with internal self-biasing provided from a charged electret foil, are good microphones to use.

Some criteria governing the actual design of the photoacoustio cell are

(1) Acoustic isolation from the outside world.

The problem of acoustic isolation is not particularly serious providing one uses lock-in detection methods for analyzing the microphone signal. One should, of course use chopping frequencies different from those present in the acoustic and vibrational spectrum present in the environment. In addition, the cell should be designed with good acoustic seals and with walls of sufficient thickness to form a good acoustic barrier. Some reasonable precautions to isolate the cell from room vibrations should also be taken.

(2) Minimization of extraneous photoacoustic signal arising from the interaction of the light beam with the walls, windows, and the microphone in the cell.

In achieving this, one should employ windows as optically transparent as possible for the wavelength region of interest, and construct the body of the cell out of polished aluminum or stainless steel. Although the walls will absorb some of the incident and scattered radiation, the resultant photoacoustic signal will be quite weak, as long as the thermal mass of these walls is large. A large thermal mass results in a small temperature rise at the surface, and thus a small photoacoustic signal. In addition, one should keep all inside surfaces clean to minimize photoacoustic signals from surface contaminats. One should also design the cell so as to minimize the amount of scattered light that can reach the microphone diaphragm.

(3) Microphone configuration.

Various microphone configurations such as cylindrical and flat can be readily used. Cylindrical microphones have the advantage of being easy to construct and have a large surface area, thereby increasing their sensitivity. A disadvantage is that they do not usually possess a flat frequency response over a wide frquency range. Flat microphones are commercially available, are quite sensitive when of reasonable size, and good quality, and flat microphone possess a flat frequency response over a wide acoustic range.

(4) Means for maximizing the acoustic signal within the cell.

Since the signal in a photoacoustic cell used for solid samples varies inversely with the gas volume (47), one should attempt to minimize the gas volume. However, one must take care not to minimize this volume to the point that the acoustic signal produced at the sample suffers appreciable dissipation to the cell window and walls before reaching the microphone. The distance between the sample and the cell window should always be greater than the thermal diffusion length of the gas, since it is this boundary layer of the gas that acts as an acoustic piston generating the signal in the cell (47). For air at room temperature and pressure, the thermal diffusion length is approximately equal to 0.02 cm at a chopping frequency of 100 Hz. In addition, one must take thermo-viscous into account as well, since this could be a source of significant signal dissipation to the cell boundaries. Thermo-viscous damping results in an $e^{-\varepsilon x}$ damping, where ε is a damping coefficient given by (48)

$$\varepsilon = (1/dv)\,(\eta_e\,\omega/2\rho_0)^{1/2}$$

where d is the closest dimension between cell boundaries in a passageway, v is the sound velocity, ω is the frequency, ρ_g is the gas density, and η_e is an effective viscosity which is dependent on both the ordinary viscosity and the thermal conductivity of the gas. Again, for air at room temperature and pressure, one finds negligible thermo-viscous damping at 100 Hz as long as d>0.01 cm. It should be noted, however, that the thermal diffusion length varies as the thermo-viscous damping coefficient varies as $(\omega)^{1/2}$. While the thermal diffusion length is a predominant factor at low frequencies, the thermo-viscous term is predominant at high frequencies. A cell that is designed to be used over a wide range of frequencies, and is capable of handling a number of

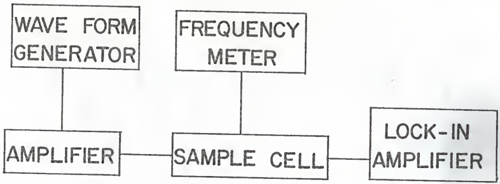

FIG. 14 BLOCK DIAGRAM OF THE EXPERIMENTAL SET-UP

gases should then have a minimum distance between the sample and window, and minimum passageway dimensions 1-2 mm.

One can further enhance the acoustic signal in the photoacoustic cell by a number of means. For example, if one need to work at only one frequency, one can take advantage of the nonflat frequency response of a cylindrical microphone and work at the frequency of its peak sensitivity. Other methods to enhance the acoustic signal include the use of gases with a higher thermal conductivity, the use of higher gas pressures, and of lower gas temperatures. The theory shows that the photoacoustic signal varies in most cases as

$$(K_g)^{1/2}(P_o)^{1/2}/T_o,$$

where K_g is the gas thermal conductivity, P_o is the pressure of the gas, and T_o is the temperature of the gas. All these methods will increase the photoacoustic signal without limiting the choice of chopping frequencies.

(5) The requirements set by the samples to be studied and the type of experiments to be performed.

How closely one adheres to the above criteria will of course depend on the type of sample used (powder, smear, liquid, etc.), its size, and of course on the type of experiment one wishes to perform (high temperature, low temperature, etc.).

C. Data Acquisition

The tasks of acquiring, storing, and displaying the data can be performed in many ways. However, certain basic procedures should be followed. For example, the signal from the microphone preamplifiershould be processed by an amplifier tuned to the chopping frequency, in order to maximize signal: noise. If phase as well as signal amplitude is desired, or if very weak signals are to be measured, then a phase-sensitive lock-in amplifier should be used. With regard to the storage and display of the data there are of course many possible schemes ranging from the relatively inexpensive chart recorder to the sophisticated minicomputer.

6.2 Physical Set-Up of Photoacoustic Apparatus

The block diagram of the experimental set-up that has been used for this thesis work is shown in Fig. 14. This set-up can be divided into three major parts such as the input to the photoacoustic cell, the experimental chamber, and the output from the cell.

The input part contains a wave form generator and

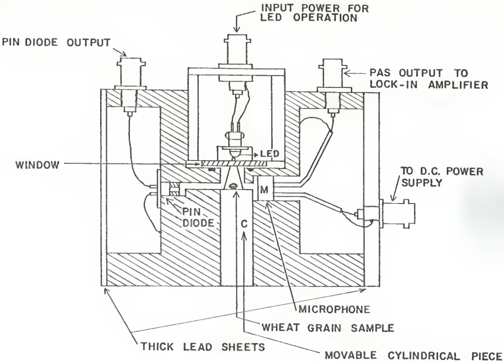

FIG. 15 PHOTOACOUSTIC CELL

an amplifier. Hewlett-Packard Model 3311A function generator was used as a wave form generator by which the chopping frequencies could be varied from 0.1-100 KHz and three kinds of wave forms could be generated namely sine, square, and ramp. The output of the waveform generator was fed as one of the inputs for the transistor power amplifier system. Power to the amplifier system was supplied by a d.c. power supply manufactured by Lambda Electronics corporation (Model LP 410 FM). This power supply could supply voltages ranging from 0-10 V and current ranges from 0-2 Amp.

The output of the power amplifier was to power the light emitting diode (LED), which was the light source in the photoacoustic cell system. The LED output was controlled by the gain of the power amplifier operated at the chopping frequency set by the function generator. Hewlett-Packard's ultra-bright lamp series HLMP-3750, -3850, -3950, and Texas Instrument's TIL-31 high power infrared LED were used as light sources for the photoacoustic cell. These devices have light outputs in the milliwatt range, comparable to small lasers, are easily modulated and cost only a few dollars.

The experimental set-up of the photoacoustic cell is shown in Fig. 15. In the design of the cell, enough care has been taken so as to satisfy the general criteria that were described in section 6.1. The main body of the cell was made out of polished aluminum and the end portions of the cell were covered with lead sheets so as to form a good acoustic barrier. The whole body of the cell was placed on a thick lead block so as to isolate it from the environmental vibrations. On the left portion of the cell, Hewlett-Packard's 5082-4200 series PIN photodiode was provided in order to monitor the light intensity of the LED source coming into the cell area. On the right portion of the cell, a Radio Shack's Archer Electret condenser mike element was used to detect the photoacoustic signal. An external d.c. bias (4.5V) was provided for the working of the microphone. The microphone element has a typical flat frequency response over a range of 20-3000 Hz. In order to have a provision for varying the cell volume, the central portion of the bottom half of the cell was made in the form of a movable cylindrical piece C. On the top portion of this piece, a small depression was made in order to keep a wheat kernel in place. Between the sample and LED source a Supersil fused quartz window, which is as optically transparent as possible in the frequency range 10-1000 Hz has been provided. In order to avoid multiple reflections within the cell the bottom portion surrounding the LED was coated with lamp black.Both the PIN-diode and the microphone were provided with BNC connectors for connection to the lock-in amplifier.

The output of the microphone was connected to an Ithaco Dynatrac 393 lock-in amplifier system in order to measure the photoacoustic signal. This lock-in amplifier responds only to those signals that are coherent with a reference frequency. It will track the frequency of an external reference with neither amplitude nor phase errors. Hence for the working of the lock-in amplifier a reference frquency signal was to be supplied from the output of the power amplifier for the LED. This particular lock-in amplifier works on the principle of heterodyning, which is a technique used commonly in ordinary radios whereby the input signal is translated or "mixed" to a fixed intermediate frequency before the signal is detected. The experimental data was analysed using the LOTUS spread sheet program in a Zenith 150 personnel computer. Various kinds of experiments and their results will be discussed in the next chapter in detail.

CHAPTER VII

EXPERIMENTAL RESULTS AND DISCUSSION

The various kinds of experiments that have been performed in order to distinguish between soft and hard varieties of wheat kernels on the basis of their photoacoustic response are discussed in this chapter. The wheat characteristics which will affect the photoacoustic signal are density, thermal conductivity, specific heat, and optical absorption coefficient.

The following parameters were kept constant for almost each experiment that was performed upon the wheat grain samples using the photoacoustic set-up described earlier.

- The d.c. supply voltage for the microphone operation was 5v.
- The time constant setting in the lock-in amplifier was 4.0 sec.
- The gas pressure inside the cell was almost contant, approximately equal to atmospheric pressure.
- The cell volume was maintained contant throughout this project.
- The function generator's amplitude was kept maximum in all the experiments that have been performed.
- Run to run maintenance was good.

(a) The cell's inner parts were thoroughly cleaned with methanol after each run in order to avoid erroneous signals coming from the surface contaminants.

(b) After placing the sample inside the cell, the cell was flushed out with helium gas for about two minutes and then the two needle valves that are attached to the main body of the cell were closed almost at the same time.

7.1 Ambient Humidity Conditions for Wheat Samples

Whenever a new experiment has to be performed on a wheat sample, or the validity of the previous results of an experiment has to be rechecked, then the starting conditions of the wheat samples should remain ideally the same in order to have a comparative idea about the experimental results. The standard procedure in obtaining this condition is described below.

A. Wheat Kernel Samples

An oven was pre-heated to a temperature of 130°C. The wheat kernels were kept individually either in an aluminum foil or in an aluminum heating dish and then were kept inside the oven for 19 hours. Once phe wheat samples were taken out of the oven, then they were kept inside a desiccator immediately in order to avoid the moisture absorption from the atmosphere. The sample was taken out of the oven just prior to use the photoacoustic set-up.

B. Powdered Wheat Samples

Two grams of wheat powder was taken and was made into a pellet by using a mechanical press. Then, these pellets were kept in an aluminum foil and kept into a preheated oven (13^{o} C) for one hour. After that they were taken out and kept inside a desiccator.

7.2 Experiments and Their Results

TEST # 1

To start with the LEDs were checked for their uniformity in exhibiting their characterisics. This was done by using a McPherson 0.3 monochromator attached with an RCA 1P28 photomultiplier tube and carrying out the scanning over a wide range of frequencies. From the obtained intensity versus wavelength plot it was found that the LEDs were quite consistent with their characteristics without much variation from one LED to another belonging to the same group.

TEST # 2

As a next step, in order to find out in which wavelength region the absorption is going to be maximum, wheat samples have been placed in the cell and their photoacoustic response was measured over the frequency range 10-1000 Hz, using each type of LED described above. In order to have a fairly good amount of measurable signal, five kernels of wheat were placed inside the cell and the data measurements were taken. Then a log-log graph was plotted taking the chopping frequency along the x-axis and the photoacoustic response (in microvolts) along the y-axis and the results of hard and soft wheat measurements were compared to see which LED should be used for the forthcoming experiments. These plots are shown in graph # 2 and 3. Of all the LEDs, the near infrared LED gave the maximum signal for both hard and soft wheats. The variation of photoacoustic response is primarily due to the light intensity from the various LEDs. The near IR LED gave the highest light output, hence the largest signal. With all the LEDs, it has been found that the signal level of soft wheat was always higher than that of hard wheat. One of the possible explanation that can be given is in terms of the thermal properties of the two varieties of the wheat. As it has been mentioned earlier, the wheat characteristics which will affect the photoacoustic signal are density, thermal conductivity, specific heat, and optical absorption coefficient. Of these four thermal properties, information is available for three of them except for the optical absorption coefficient. Some typical values are given in table 2 (50,51).

TABLE 2 Thermal Properties of Wheat Samples.

Wheat Variety	Density	Specific Heat Btu per lb deg F	Thermal cond. Btu/hr ft deg F
Hard	1.30	0.370	0.0810
Soft	1.32	0.334	0.0676

As the theory indicates (46, 47), the photoacoustic effect is primarily dependent on the relationship between three "length" parameters of the sample: The actual thickness of the sample l, the optical absorption length $\ell_\beta = 1/\beta$ where β is the optical absorption coefficient, and the thermal diffusion length $\mu = (2\alpha/\omega)^{\frac{1}{2}}$, where α is the thermal diffusivity, ($\alpha = \kappa/\ell C$,k is the thermal conductivity, ω is the density, and C is the specific heat) and is the chopping frequency. According to the two cases of optically opaque (thick) solids,

(1) Thermally thick solids ($\mu < \ell$; $\mu > \ell_\beta$) , and

(2) Thermally thick solids ($\mu << \ell$; $\mu < \ell_\beta$

the slope of the log-log plots drawn between frequncy versus photoacoustic signal is going to change. In the first case, the parameter dependence is going to be like

$$Q \; \alpha \; (\ell \kappa C)^{-\frac{1}{2}}$$

i.e. The signal varies inversely as the square root of ℓ, k, and C.

In the second case the signal looks like

$$Q \; \alpha \; \beta/\ell C$$

i.e. now the signal is independent of k, but is dependent on a new factor namely the optical coefficient β. In this case, the signal varies inversely with C, and ℓ.

So from the above short review and by looking at Table 7.1, the signal of soft wheat should higher in both the cases in spite of the fact that the soft wheat has a slightly lower density than the hard wheat. This is much compensated by the higher value of thermal conductivity and specific heat. If the optical absorption coefficient for the wheat were available, then the discussion can be made much more convincingly.

TEST # 3

Before proceeding further, in order to cross check that the photoacoustic cell was working properly studies were made on a black paper sample. From the reference 52, where a plot of the photoacoustic signal for carbon black has been plotted, it is quite convincing that the cell was working properly. In the graph # 1, 1/frequency dependence line has been drawn and it is quite parallel to the experimental curve. This test has been repeated twice and the scattering of the data was totally insignificant.

TEST # 4

In order to determine the reproducibility of the experiments with this photoacoustic cell, several runs were performed with five wheat kernels at a time using red LED as the source. Graphs 4, and 5 represent these runs respectively for soft and hard wheat kernels with higher signal for soft wheat. The scattering of data for hard wheat is higher than for soft wheat.

TEST # 5

The infrared LED produced a signal high enough so as to make measurements on single kernel of wheat possible. Just to have an idea for the change in signal level graph # 6 was plotted for the soft wheat kernel. Again to see how much these results are reproducible, several runs of hard and soft wheat single kernel measurement were carried out using the infrared LED as the source. These plots are being shown in graph #s 7 and 8. The data for soft wheat was quite reproducible whereas the scattering of data for the hard wheat was more as in the previous case. The fact that we observed more scatter using both the near IR and red LEDs, may indicate that there is more kernel-to-kernel variability in the hard wheat.

TEST # 6

Several studies were carried out by exposing the wheat to different humidity conditions and observing the effects of moisture on the photoacoustic response of wheat samples. Humidity chambers of Relative Humidity (RH) 30 %, and 90 % were made by mixing water and glycerine in the proper proportions (53). The wheat samples (5 kernels each) were taken out of the desiccator, and kept in the 30 % humidity chamber for 24 hours. Then they were put into the photoacoustic cell and by varying the chopping frequency, the signal from the microphone was noted continuously. These plots together with plots of the photoacoustic response of the dried wheat are shown in graph #s 9, and 10. The graph for RH 30 % condition has a lower photoacoustic signal value than that for the dried wheat. This can be explained from the fact that when the wheat is exposed to a higher relative humidity it absorbs moisture and because of this excess water content the specific heat and the thermal conductivity values are higher depending upon the amount of moisture that has been absorbed. Since the signal strength is inversely proportional to the specific heat and thermal conductivity values the signal strength goes down in the presence of moisture.

A comparison of five kernel versus single kernel studies for the hard wheat exposed to RH 30 % chamber has been shown in graph 11. In this case also, exposure to moisture gives a lower signal value.

TEST # 7

In the transmission electron micrographs of the hard wheat sample (section 4.2), there was some void space in between the starch cells and the protein matrix whereas for the soft wheat sample there were no such voids. This created a fundamental doubt that during the preparation of the TEM specimen, both the varieties of wheat undergo some kind of chemical and internal structural changes. It appears that in the case of soft wheat it regains its original form in a much quicker time than hard wheat and hence there is no void in between the starch cell and the protein matrix. This makes one feel that the soft wheat reacts at a faster rate to any environmental changes. In order to make sure about this particular factor, both the wheat varieties were kept in separate RH 90 % humidity chambers on different dates, to study the rate of moisture absorption. For both the varieties, each time only one kernel was taken off after some intervals like 0.5 hour, 1 hour, 2 hours, etc., and the photoacoustic response versus chopping frequency curves were studied. For the soft wheat, the absorption was close to saturation after the end of twelfth hour, and hence the experiment was stopped at the end of fifteenth hour. In the case of hard wheat even after two hours of exposure there is not much of a difference in the signal levels and hence the kernel was taken off from the humidity chamber after seven hours of exposure and the experiment was continued so on so forth. For the hard wheat, the saturation was approached only after a period of 34 hours. Graph #s 12, and 13 gives a step-by-step moisture absorption for the soft wheat whereas graph #s 15, and 16 show similar results for the hard wheat. Graph #s 14, and 17 represent the complete cycle of moisture study for the soft and hard wheat respectively.

This particular study clearly indicates that the soft wheat absorbs moisture at a rate faster than the hard wheat and it may give an explanation for the TEM photographs of voids in the hard wheat's microscopic structure.

Graph #s 18, 19, and 20 were plotted for time of exposure of the sample in the humidity chamber versus photoacoustic signal corresponding to the fixed frequencies 1000 Hz, 100 Hz, and 10Hz respectively. In the first two graphs (18 and 19) the change in the signal is quite steep, but the saturation level couldnot occur for quite a long time, whereas at 10 Hz frequency both the curves attain saturation at a much fater rate.

Graph 1 - A log-log plot of the photo-acoustic signal versus chopping frequency for the black paper sample using an infrared LED as the source.

symbol descriptions:

square	Run #1
plus	Run #2

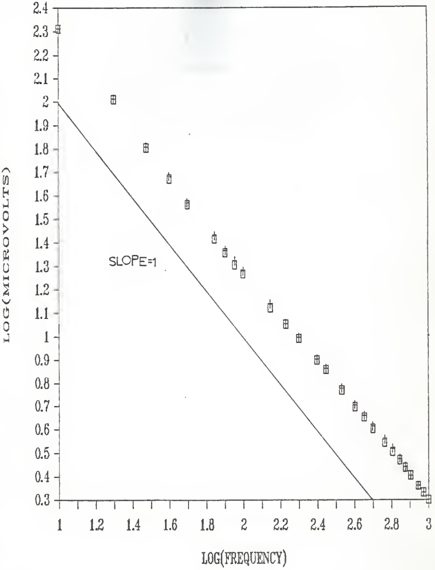
2.4
2.3
2.2
2.1
2
1.9
1.8
1.7
1.6
1.5
1.4
1.3
1.2
1.1
1
0.9
0.8
0.7
0.6
0.5
0.4
0.3
LOG(MICROVOLTS)
SLOPE=1
1
1.2
1.4
1.6
1.8
2
2.2
2.4
2.6
2.8
3
LOG(FREQUENCY)

Graph 2 - A log-log plot of the photo-acoustic signal versus chopping frequency for five kernels of soft wheat using different coloured LEDS as the sources.

symbol description:

square	Near Infra-Red
plus	Red
diamond	Green
triangle	Yellow

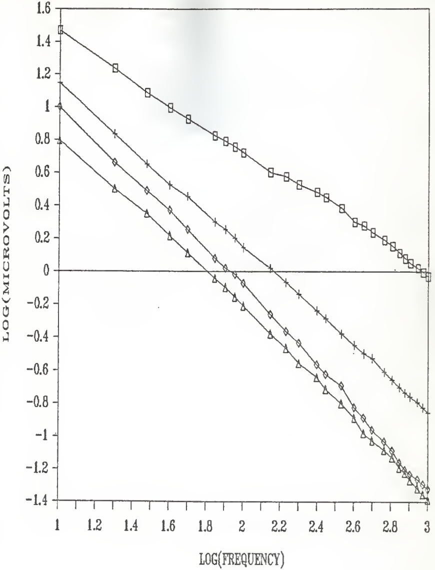
1.6
1.4
1.2
1
0.8
0.6
0.4
0.2
0
-0.2
-0.4
-0.6
-0.8
-1
-1.2
-1.4
LOG(MICROVOLTS)
1
1.2
1.4
1.6
1.8
2
2.2
2.4
2.6
2.8
3
LOG(FREQUENCY)

Graph 3 - A log-log plot of the photo-acoustic signal versus chopping frequency for five kernels of hard wheat sample using different coloured LEDS as the sources.

symbol description:

square	Near Infra-Red
plus	Red
diamond	Green
triangle	Yellow

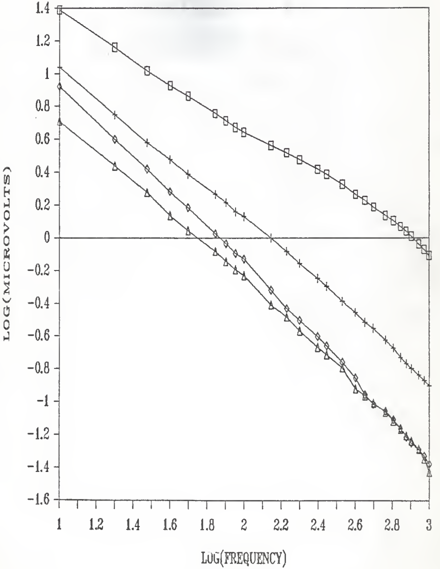

LOG(MICROVOLTS)
1.4
1.2
1
0.8
0.6
0.4
0.2
0
-0.2
-0.4
-0.6
-0.8
-1
-1.2
-1.4
-1.6
1
1.2
1.4
1.6
1.8
2
2.2
2.4
2.6
2.8
3
LOG(FREQUENCY)

Graph 4 - A log-log plot of the photo-acoustic signal versus chopping frequency for five kernels of soft wheat sample using a Red LED as the source of incident radiation.
(A check for reproducibility and consistency of the experimental results)

symbol description:

square	Group #4, Run#4
plus	Group#4, Run#5
diamond	Group #4, Run#6
triangle	Group #4, Run#7
cross	Group #4, Run#8
inverted triangle	group #4, Run#9

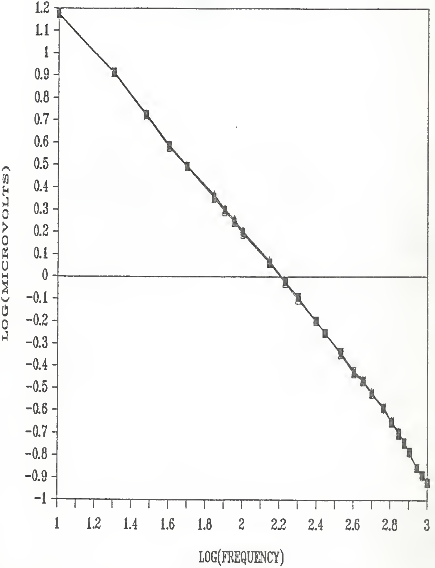
LOG(MICROVOLTS)
1.2
1.1
1
0.9
0.8
0.7
0.6
0.5
0.4
0.3
0.2
0.1
0
-0.1
-0.2
-0.3
-0.4
-0.5
-0.6
-0.7
-0.8
-0.9
-1
1
1.2
1.4
1.6
1.8
2
2.2
2.4
2.6
2.8
3
LOG(FREQUENCY)

Graph 5 - A log-log plot of the photo-acoustic signal versus chopping frequency for five kernels of hard wheat sample using a Red LED as the source of incident radiation.
(A check for reproducibility and consistency of the experimental results)

symbol description:

square	Group #4, Run#4
plus	Group #4, Run#5
diamond	Group #4, Run#6
triangle	Group #4, Run#7
inverted triangle	Group #4, Run#9

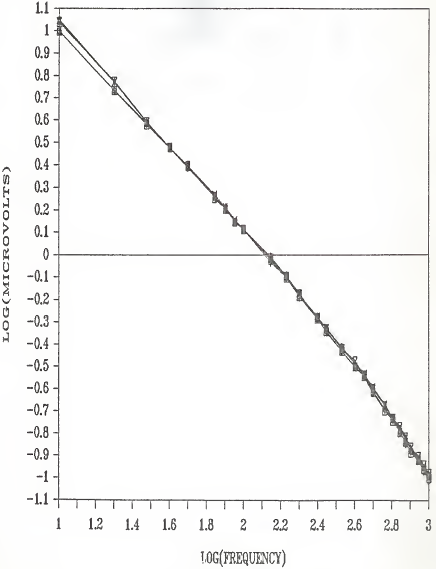

LOG(MICROVOLTS)
LOG(FREQUENCY)

Graph 6 - A log-log plot of the photo-acoustic signal versus chopping frequency for a wheat single kernel compare with five kernels of soft wheat using an Infra-Red LED as the source of incident radiation.

symbol description:

square	Five kernels, Group#2, Run#1
plus	single kernel,Group#1, Run#1

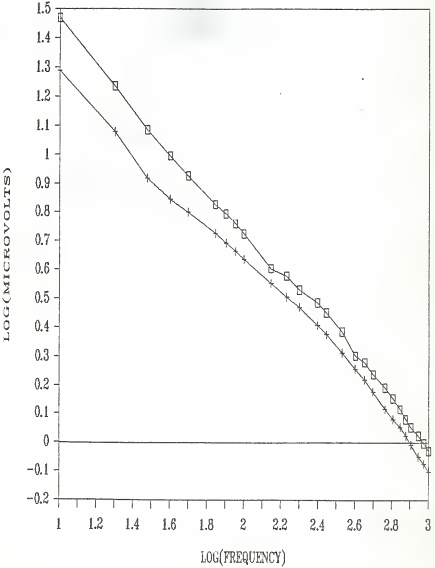

1.5
1.4
1.3
1.2
1.1
1
0.9
0.8
0.7
0.6
0.5
0.4
0.3
0.2
0.1
0
-0.1
-0.2
LOG(MICROVOLTS)
1
1.2
1.4
1.6
1.8
2
2.2
2.4
2.6
2.8
3
LOG(FREQUENCY)

Graph 7 - A log-log plot of the photo acoustic signal versus chopping frequency for soft wheat single kernels using an Infra-Red LED as the source. (A check for reproducibility of the experimental results)

Symbol Description:

suqare	Group #1, Run #1
plus	Group #1, Run #2
diamond	Group #2, Run #1
triangle	Group #3, Run #1
cross	Group #4, Run #1

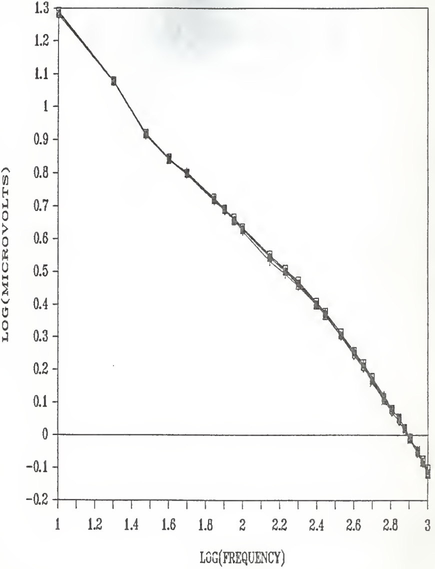
1.3
1.2
1.1
1
0.9
0.8
0.7
0.6
0.5
0.4
0.3
0.2
0.1
0
-0.1
-0.2
LOG(MICROVOLTS)
1
1.2
1.4
1.6
1.8
2
2.2
2.4
2.6
2.8
3
LOG(FREQUENCY)

Graph 8 - A log-log plot of the photo-acoustic signal versus chopping frequency for hard wheat single kernels using an Infra-Red LED as the source.

Symbol Description:

square	Group #1, Run #1
plus	Group #1, Run #2
diamond	Group #2, Run #1
triangle	Group #3, Run #1
cross	Group #4, Run #1

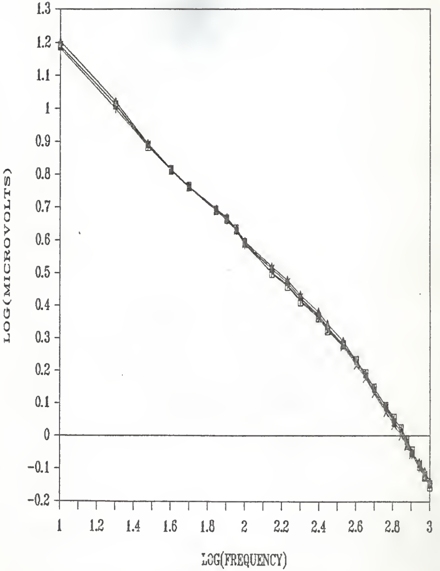
1.3
1.2
1.1
1
0.9
0.8
0.7
0.6
0.5
0.4
0.3
0.2
0.1
0
-0.1
-0.2
LOG(MICROVOLTS)
1
1.2
1.4
1.6
1.8
2
2.2
2.4
2.6
2.8
3
LOG(FREQUENCY)

Graph 9 - A log-log plot of the photo-acoustic signal versus chopping frequency for soft wheat kernels at different relative humidities (RH) using an Infra-Red LED as the source.

Symbol Description:

square	Five kernels, Group #2, Run #1 (Ambient (Ambient Humidity)
plus	Five kernels, Group #2, Run #1 (RH 30%)
diamond	Single kernel, Group #2, Run #1 (Ambient Humidity)
triangle	Single kernel, Group #2, Run #1 (RH 30%)

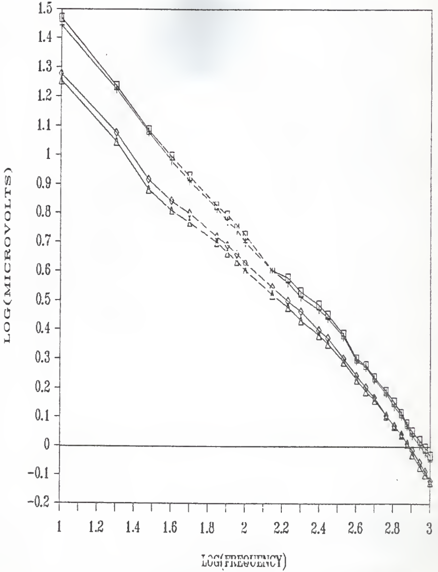

1.5
1.4
1.3
1.2
1.1
1
0.9
0.8
0.7
0.6
0.5
0.4
0.3
0.2
0.1
0
-0.1
-0.2
LOG(MICROVOLTS)
1
1.2
1.4
1.6
1.8
2
2.2
2.4
2.6
2.8
3
LOG(FREQUENCY)

Graph 10 - A log-log plot of the photo-acoustic signal versus chopping frequency for hard wheat kernels at different relative humidities using an infrared LED as the source.

symbol description:

square	Five kernels, Group#2, Run#1(ambient humidity)
plus	Five kernels, Group#2, Ru-#1(RH30%)
diamond	Single kernel, Group#2, Run#1(Ambient Humidity)
triangle	Single kernel, Group#2, Run#1(RH30%)

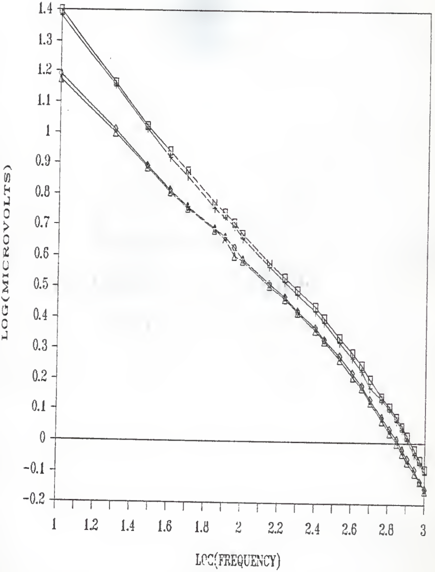
LOG(MICROVOLTS)
1.4
1.3
1.2
1.1
1
0.9
0.8
0.7
0.6
0.5
0.4
0.3
0.2
0.1
0
-0.1
-0.2
1
1.2
1.4
1.6
1.8
2
2.2
2.4
2.6
2.8
3
LOG(FREQUENCY)

Graph 11 - A log-log plot of the photo-acoustic signal versus chopping frequency for hard wheat (RH30%) using an Infra-Red LED as the source.

symbol description:

square	Five kernels, Group#1, Run#1
plus	Five kernels, Group#2, Run#1
diamond	Five kernels, Group#3, Run#1
triangle	Single kernel, Group#1, Run#1
cross	Single kernel, Group#2, Run#1
inverted triangle	Single kernel, Group#3, Run#1

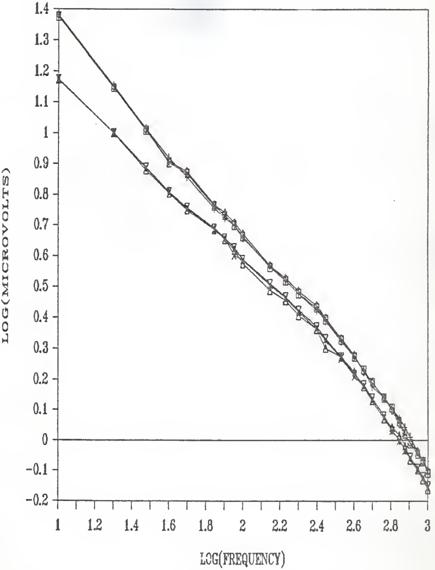
LOG(MICROVOLTS)
1.4
1.3
1.2
1.1
1
0.9
0.8
0.7
0.6
0.5
0.4
0.3
0.2
0.1
0
-0.1
-0.2
1
1.2
1.4
1.6
1.8
2
2.2
2.4
2.6
2.8
3
LOG(FREQUENCY)

Graph 12 - A log-log plot of the photo-acoustic signal versus chopping frequency for single kernel soft wheat (RH90%) using an Infra-Red LED as the source.

Time factor study (0-7 hrs) for the rate of moisture absorption, starting from the Ambient Humidity condition.

symbol desription:

square	0hr
plus	0.5hr
diamond	1hr
triangle	2hrs
cross	3hrs
inverted tiangle	7hrs

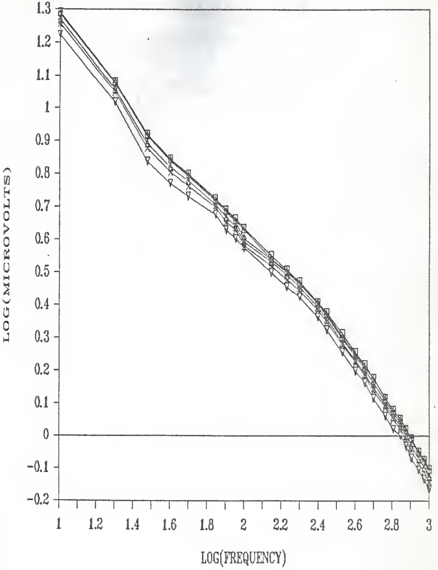

1.3
1.2
1.1
1
0.9
0.8
0.7
0.6
0.5
0.4
0.3
0.2
0.1
0
-0.1
-0.2
LOG(MICROVOLTS)
1
1.2
1.4
1.6
1.8
2
2.2
2.4
2.6
2.8
3
LOG(FREQUENCY)

Graph 13 - A log-log plot of the photo-acoustic signal versus chopping frequency for single kernel soft wheat (RH90%) using an Infra-RED led as the source.

Time factor study (3-15 hrs)for the rate of moisture absorption.

symbol description:

square	3 hrs
plus	7 hrs
diamond	10 hrs
cross	13 hrs
inverted triangle	15 hrs

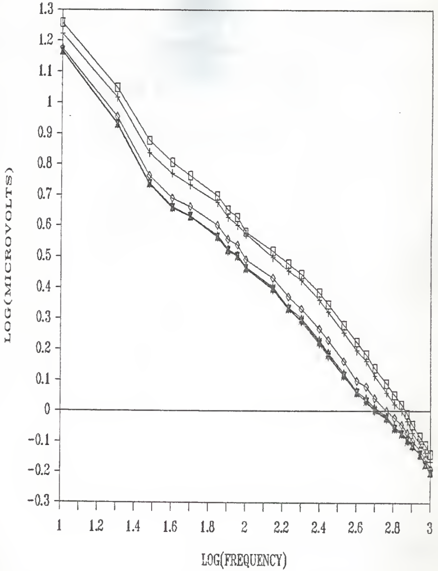
1.3
1.2
1.1
1
0.9
0.8
0.7
0.6
0.5
0.4
0.3
0.2
0.1
0
-0.1
-0.2
-0.3
LOG(MICROVOLTS)
1
1.2
1.4
1.6
1.8
2
2.2
2.4
2.6
2.8
3
LOG(FREQUENCY)

Graph 14 - A log-log plot of the photo-acoustic signal versus chopping frequency for single kernel soft wheat (RH90%) using an Infra-Red LED source. Time factor study (0-15hrs) for the rate of moisture absorption, starting from the ambient humidity condition to the saturation level of absorption.

symbol description:

square	0 hr
plus	2 hrs
diamond	7 hrs
triangle	10 hrs
cross	12 hrs
inverted triangle	15 hrs

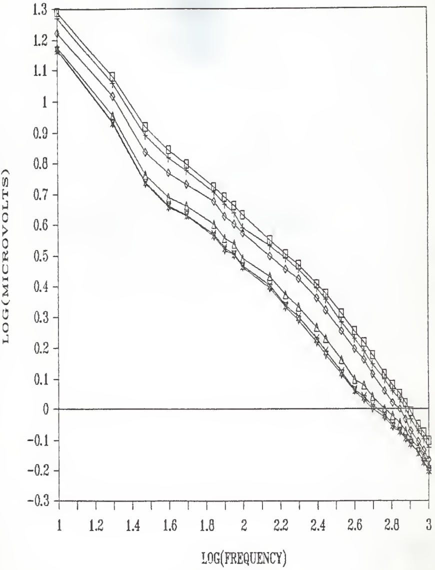
1.3
1.2
1.1
1
0.9
0.8
0.7
0.6
0.5
0.4
0.3
0.2
0.1
0
-0.1
-0.2
-0.3
LOG(MICROVOLTS)
1
1.2
1.4
1.6
1.8
2
2.2
2.4
2.6
2.8
3
LOG(FREQUENCY)

Graph 15 - A log-log plot of the photo-acoustic signal versus chopping frequency for single kernel hard wheat (RH90%) using an Infra-Red LED as the source. Time factor study (0-11 hrs) for the rate of moisture absorption, starting from the ambient humidity condition.

symbol description:

square	0 hr
plus	1 hr
diamond	2 hrs
triangle	4 hrs
cross	7 hrs
inverted triangle	11 hrs

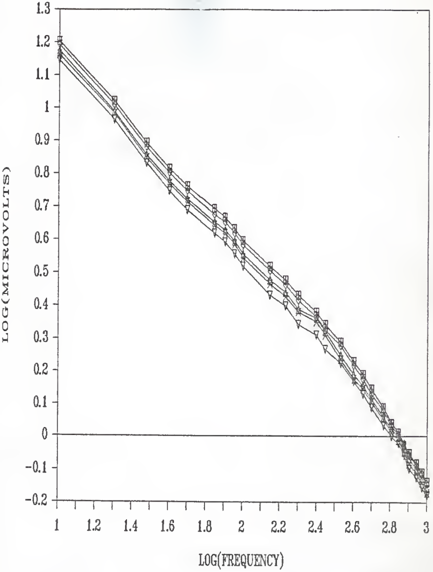
1.3
1.2
1.1
1
0.9
0.8
0.7
0.6
0.5
0.4
0.3
0.2
0.1
0
-0.1
-0.2
LOG(MICROVOLTS)
1
1.2
1.4
1.6
1.8
2
2.2
2.4
2.6
2.8
3
LOG(FREQUENCY)

Graph 16 - A log-log plot of the photo-acoustic signal versus chopping frequency for a single kernel hard wheat (RH 90%) using an Infra-Red LED as the source.
Time factor study (11-38 hrs) for the rate of moisture absorption.

symbol description:

square	11 hrs
plus	16 hrs
diamond	23 hrs
triangle	30 hrs
cross	34 hrs
inverted triangle	38 hrs

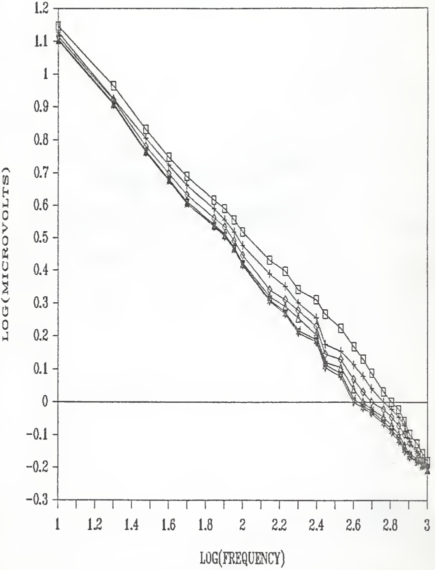
1.2
1.1
1
0.9
0.8
0.7
0.6
0.5
0.4
0.3
0.2
0.1
0
-0.1
-0.2
-0.3
LOG(MICROVOLTS)
1
1.2
1.4
1.6
1.8
2
2.2
2.4
2.6
2.8
3
LOG(FREQUENCY)

Graph 17 - A log-log plot of the photo-acoustic signal versus chopping frequency for single kernel hard wheat (RH 90%) using an Infra_Red LED as the source.

Time factor study (1-38 hrs) for the rate of moisture absorption.

symbol description:

square	1 hr
plus	4 hrs
diamond	11 hrs
triangle	23 hrs
cross	34 hrs
inverted triangle	38 hrs

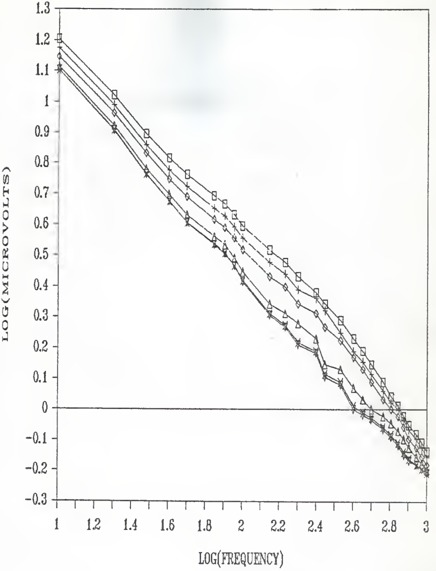
1.3
1.2
1.1
1
0.9
0.8
0.7
0.6
0.5
0.4
0.3
0.2
0.1
0
-0.1
-0.2
-0.3
LOG(MICROVOLTS)
1
1.2
1.4
1.6
1.8
2
2.2
2.4
2.6
2.8
3
LOG(FREQUENCY)

Graph 18 - A plot of the photo-acoustic signal versus time for single kernels of soft and hard wheat (Realitive Humidity-90%) at constant frequency 1000hz.

symbol description:

square	soft wheat sample
plus	hard wheat sample

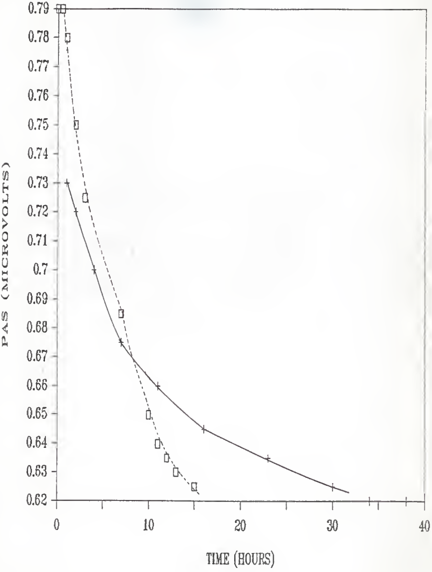

PAS (MICROVOLTS)
0.79
0.78
0.77
0.76
0.75
0.74
0.73
0.72
0.71
0.7
0.69
0.68
0.67
0.66
0.65
0.64
0.63
0.62
0
10
20
30
40
TIME (HOURS)

Graph 19 - A plot of the photo-acoustic signal versus time for single kernels of soft and hard wheat (Realitive Humidity 90%) at constant frequency 100 Hz

symbol description:

square	soft wheat sample
plus	Hard wheat sample

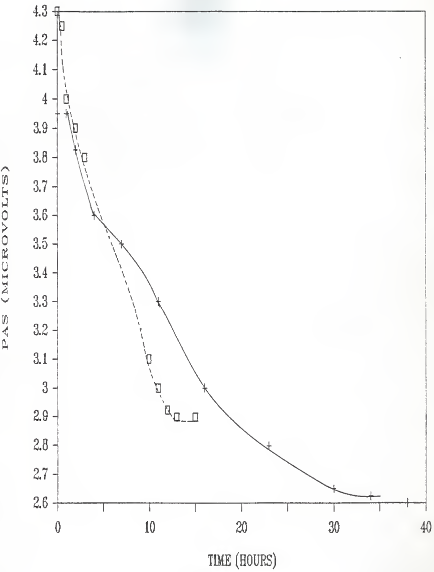
PAS (MICROVOLTS)
4.3
4.2
4.1
4
3.9
3.8
3.7
3.6
3.5
3.4
3.3
3.2
3.1
3
2.9
2.8
2.7
2.6
0
10
20
30
40
TIME (HOURS)

Graph 20 - A plot of the photo-acoustic signal versus time for single kernels of soft and hard wheat (Humidity 90%) at constant frequency 10 Hz.

symbol description:

square	11 hrs
plus	16 hrs
diamond	23 hrs
triangle	30 hrs
cross	34 hrs
inverted triangle	38 hrs

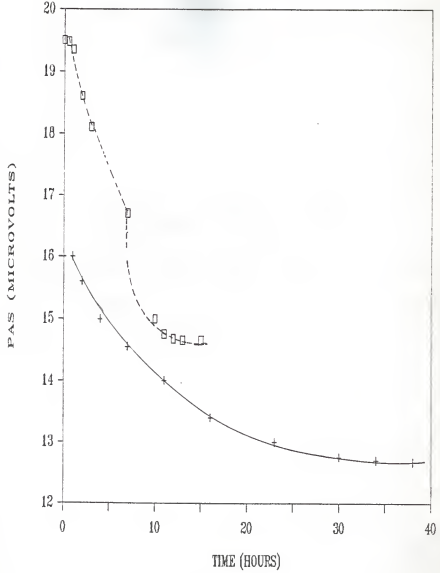

20
19
18
17
16
15
14
13
12
PAS (MICROVOLTS)
0
10
20
30
40
TIME (HOURS)

Graph 21 - A log-log plot for the photo- acoustic signal versus chopping frequency for single kernel soft and hard wheat with orientations, using an Infra-Red LED as the source.

symbol description:

square	Incident radiation falls directly on the crease of the soft wheat kernel.
plus	Incident radiation does not fall directly on the crease of the soft wheat kernel.
diamond	Incident radiation falls directly on the crease of the hard wheat kernel.
triangle	Incident radiation does not fall directly on the crease of the hard wheat kernel.

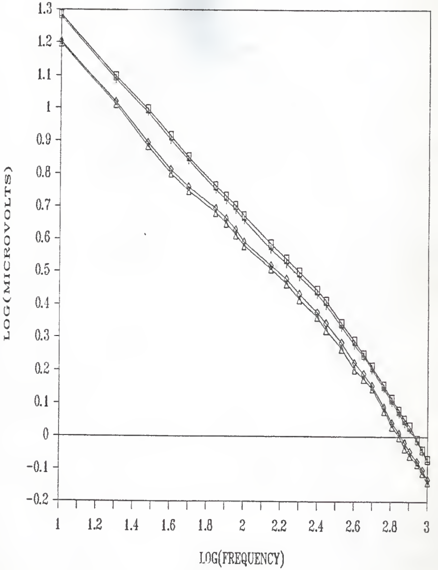
1.3
1.2
1.1
1
0.9
0.8
0.7
0.6
0.5
0.4
0.3
0.2
0.1
0
-0.1
-0.2
LOG(MICROVOLTS)
1
1.2
1.4
1.6
1.8
2
2.2
2.4
2.6
2.8
3
LOG(FREQUENCY)

Graph 22 - A log-log plot of the photo-acoustic signal versus chopping frequency for soft wheat flour (pressed into a pellet form) using an Infra-Red as the source. (A check for reproducibility of experimental results).

symbol description:

square	Group#1, Run#1
plus	Group#1, Run#3
diamond	Group#1, Run#4
triangle	Group#2, Run#2
cross	Group#2, Run#3
inverted triangle	Group#2, Run#4

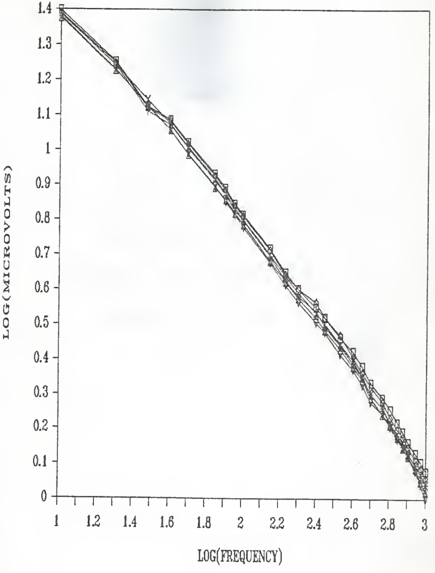
LOG(MICROVOLTS)
1.4
1.3
1.2
1.1
1
0.9
0.8
0.7
0.6
0.5
0.4
0.3
0.2
0.1
0
1
1.2
1.4
1.6
1.8
2
2.2
2.4
2.6
2.8
3
LOG(FREQUENCY)

Graph 23 - A log-log plot of the photo-acoustic signal versus chopping frequency for hard wheat flour (pressed into a pellet form) using an Infra-Red LED as the source.

symbol description:

square	Group#1, Run#1
plus	Group#1, Run#3
diamond	Group#1, Run#4
triangle	Group#2, Run#1
cross	Group#2, Run#2
inverted triangle	Group#2, Run#4

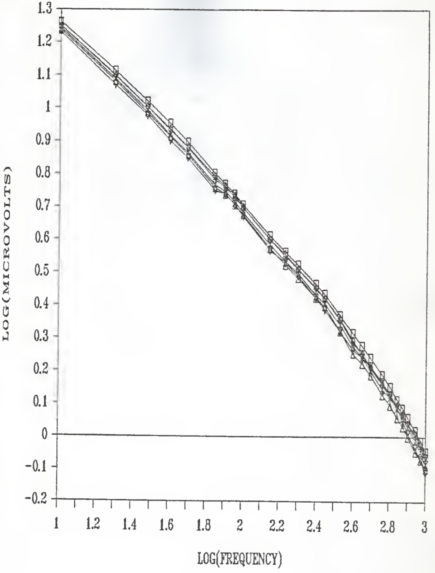

1.3
1.2
1.1
1
0.9
0.8
0.7
0.6
0.5
0.4
0.3
0.2
0.1
0
-0.1
-0.2
LOG(MICROVOLTS)
1
1.2
1.4
1.6
1.8
2
2.2
2.4
2.6
2.8
3
LOG(FREQUENCY)

TEST # 8

From the cross-section diagram of the wheat kernel it is quite clear that the internal structure of wheat is not uniform throughout and hence it creates a question of whether the photoacoustic signal changes with the kernel orientation. so in order to make things clear, a kernel orientation study was carried out. The kernel was exposed at two different orientations to the incoming radiation given out by the IR LED and it was found that there was not much of a difference in the photoacoustic signals. A possible explanation might be as follows. The wheat kernel has a uniform outer layer known as bran and during the depth profiling by varying the modulation frequency, we might not have gone below this layer and hence we might not have got any change in the signal with respect to the orientation.

TEST # 9

In order to study the differences between the whole wheat kernels and the powdered samples in their photoacoustic response, pellets were made out of the powdered samples using a mechanical press. 1 hour, 130° C heat treatment was given to dry these pellets and the usual photoacoustic curve was taken for several runs of hard and soft wheat pellets. The curves are drawn in graph #s 22, and 23. In this case also, soft wheat pellets had a higher signal value than the hard ones but with more scattering of data from run to run. Of course, in this case since both the varieties are uniformly pressed into a pellet form more or less they shoud have uniform densities and hence the change in signal level between the two varieties should have to be accounted only through the other three parameters.

7.3 Conclusions

Taking a typical hard and a typical soft variety of wheat, different experiments have been carried out in differentiating the two varieties from their photoacoustic response. We were consistently able to differentiate between the particular hard and soft varieties we tested, both on the basis of their photoacoustic response and on their rate of moisture absorption. The results of the moisture absorption study may give an explanation for the transmission electron micrographs.

LIST OF REFERENCES

(1) AITKEN, T. R., and ANDERSON, J. A. Conflicting opinions on the quality of bread wheats. Trans. Am. Assoc. Cereal Chemists. 5: 6-18 (1947).

(2) LARMOUR, R. K., WORKING, E. B., and OFELT, C. W. Quality tests on hard red winter wheats. Cereal Chem. 16: 733-752 (1939).

(3) KENT-JONES, D. W., and AMOS, A. J. Modern Cereal Chemistry. The Northern Publishing Company: Liverpool (1947).

(4) PERCIVAL, J. The Wheat Plant. Dutton: New York (1921).

(5) KENT, N. L. Technology of cereals with special reference to wheat. Pergamon press. pp.65 (1966).

(6) SHELLENBERGER, J. A. Wheat: Chemistry and Technology. pp.2 (1971).

(7) SWANSON, C. O. Wheat flour and quality. Burgess Publishing Company. pp.51 (1941).

(8) HEHN, E. R., and BARMORE, M. A. Breeding wheat for quality. Advan. Agron. 17 : 85 (1965).

(9) BYRON S. MILLER, and JOHN A. JOHNSON. A review of methods for determining the quality of wheat and flour for bread making. Kansan Agri. Exp. Sta. Tech. Bull. (1976).

(10) LAWRENCE ZELENY. Criteria of wheat quality. Wheat Chemistry and Technology. pp.20 (1971).

(11) REITZ, L. P., and BRIGGLE, L. W. Distribution of the varieties and classes of wheat in the U.S. in 1964. U.S. Dept. of Agriculture, Agricultural Research Service Stat. Bull. # 369 (1966).

(12) HLYNKA, I., and BUSHUK, W. The weight per bushel. Cereal Sci. Today. 4 : 239 (1959).

(13) SHUEY, W.C., A wheat sizing technique for predicting flour milling yield. Cereal Sci. Today. 5 : 71 (1960).

(14) American Association of Cereal Chemists. Approved methods of the AACC. The Association. : St.Paul, Minn. (1962).

(15) U.S. Dept. of Agriculture. Methods for determining the moisture content as specified in the official Grain standards of the U.S. and in U.S. standards for beans ,peas, lentils, and rice. Agricultural Marketing Service, Serv. & Reg. Announcement # 147 (Rev. 1959).

(16) LAWRENCE ZELENY. Wheat: Chemistry and Technology. pp.30 (1971).

(17) JONES, D. B. A new factor for converting the percentage of nitrogen in wheat into that of protein. Cereal Chem. 3 : 194-198 (1926).

(18) AAMODT, O. S., and TORRIE, J. H. Studies on the inheritance of and the relationship between kernel texture and protein content in several spring wheat crosses. Can. J. Res. Sect. C. 13 : 202 (1935).

(19) BIFFIN, R. H. Mendel's law of inheritance and wheat breeding. J. Agric. Sci. England. 1 : 4 (1905).
(20) TAYLOR, J. W., BAYLES, B. B., and FIFIELD C. C. A simple measure of kernel hardness in wheat. J. Am. Soc. Agron. 31 : 775-784 (1939).
(21) McCLUGGAGE, M. E. Factors influencing the pearling test for kernel hardness in wheat. Cereal Chem. 20 : 686-700 (1943).
(22) BAYLES, B. B. Determining utility values of wheat varieties. Milling Production. 14 (8) : 10-12 (1949).
(23) SWANSON, C. O. Cereal chemistry for operative millers : Wheat properties judged by utility value. Milling Production. 12 (9) : 8-9 (1947).
(24) BERG, S. O. Is the degree of grittiness of wheat flour mainly a varietal character ? Cereal Chem. 24 : 274-283 (1947).
(25) CUTLER, G. H., and WORZELLA, W. W. The wheat meal fermentation time test of "Quality" in wheat as adapted for small plant breeding samples. Cereal Chem. 10 : 250-262 (1933).
(26) GROSH, G. M., and MILNER, M. Cereal Chem. 36 : 260 (1959).
(27) KATZ, R., CARDWELL, A. B., COLLINS, N. D., and HOSTETTER, A. E. Cereal Chem. 36 : 393 (1959).
(28) American Association of Cereal Chemists. Cereal laboratory methods (7th ed.) The Association : St.Paul, Minn.
(29) YAMAZAKI, W. T., and DONELSON, J. R. Kernel hardness of some U.S. wheats. Cereal Chem. 60 : 344-349 (1983).
(30) STENVERT, N. L. Grinding resistance. A simple measure of wheat hardness. Flour Anim. Feed Milling. 7 : 24 (1974).
(31) CHUNG, C.H., CLARK, S.J., LINDHOLM, J.C., McGINTY, R.J., and WATSON, C.A. The pearlograph technique for measuring wheat hardness. Trans. ASAE. 18 : 185 (1975).
(32) OBUCHOWSKI, W., AND BUSHUK, W. Wheat hardness: Comparison of methods of its evaluation. Cereal Chem. 57 : 421-425 (1980).
(33) BRADBURY, D., CULL, I. M., and MacMASTERS, M. M. Structure of the mature wheat kernel. I. Gross anatomy and relationships of parts. Cereal Chem. 33 : 329-342 (1956).
(34) BRADBURY, D., MacMASTERS, M. M., and CULL, I. M. II. Microscopic structure of pericarp, seed coat, and other coverings of the endosperm and germ of hard red winter wheat. Cereal Chem. 33 : 342-360 (1956).
(35) BRADBURY, D., MacMASTERS, M. M., and CULL, I. M. III. Microscopic structure of the endosperm of hard red winter wheat. Cereal Chem. 33 : 361-373 (1956).
(36) BRADBURY, D., MacMASTERS, M. M., and CULL, I. M. IV. Microscopic structure of the germ of hard red winter wheat. Cereal Chem. 33 : 373-391 (1956).

(37) MacMASTERS, M. M., HINTON, J. J. C., and BRADBURY, D. Microscopic structure and composition of the wheat kernel. In Wheat Chemistry and Technology, V. Pomeranz (Editor). American Association Cereal Chemistry, Inc., St.Paul, Minn.
(38) KENT, N. L. Subaleurone cells of high protein content. Cereal Chem. 43 : 585-601 (1966).
(39) HOSENEY, R. C., and SEIB, P. A. Structural differences in hard and soft wheat. The Bakers Digest. pp.26 (1973).
(40) BARLOW, K. K., and SIMMONDS, D. H. Proc. Roy. Aust. Chem. Inst. Cereal Chem. Division, 22nd Annual Conference (1972).
(41) BARLOW, K. K., and SIMMONDS, D. H. Proc. Roy. Aust. Biochem. Soc. 5 : 37 (1972).
(42) WRIGLEY, C. W. Cereal Sci. Today. 17 : 370 (1972).
(43) ROSENCWAIG, A. Opt. Commun. 7 : 305 (1973).
(44) ROSENCWAIG, A. Anal. Chem., 47 : 592A (1975).
(45) ROSENCWAIG, A. In Advances in Electronics and Electron Physics, Academic Press, New York. 46 : 207-311 (1978).
(46) BELL, A. G. Philos. Mag. 11 : 510 (1881).
(47) ROSENCWAIG, A., and GERSHO, A. J. Appl. Phys. 47 : 64 (1976).
(48) ROSENCWAIG, A., and GERSHO, A. Science. 190 : 556 (1975).
(49) KINSLER, L. E., and FREY, A. R. Fundamentals of Acoustics (Wiley, New York), Chap. 9 (1962).
(50) ASAE Data: ASAE D243.2 Agricultural Engineers Yearbook of Standards. pp-294 (1983).
(51) ASAE Data: ASAE D243.2 Agricultural Engineers Yearbook of Standards. pp-296 (1983).
(52) ROSENCWAIG, A. Photoacoustic spectroscopy of solids. Rev. Sci. Instrum., 48 : 1133-1137 (1977).
(53) SETHNA, P. P. Ph.D. Thesis, Kansas State University, pp. 54 (1975).

PHOTOACOUSTIC CHARACTERIZATION OF WHEAT KERNELS

by

VISWANATHAN VENKATARAMAN

B.Sc., Madurai Kamaraj University, India, 1979
M.Sc., Madurai Kamaraj University, India, 1981
M. Tech., I.I.T., New Delhi, India, 1983

AN ABSTRACT OF A MASTER'S THESIS

submitted in partial fulfillment of the

requirements for the degree

MASTER OF SCIENCE

Department of Physics

KANSAS STATE UNIVERSITY
Manhattan, Kansas

1985

ABSTRACT

When a modulated light beam strikes an absorbing interface between a solid surface and a gas, an acoustic signal is produced in the gas at the same frequency as the modulation frequency. The strength of the acoustic signal depends on the amount of energy that is absorbed from the beam and the thermal properties of the absorbing surface and the gas. This effect is called the photoacoustic effect.

In this project, experiments were carried out in order to distinguish between typical hard and typical soft varieties of wheat kernels on the basis of their photoacoustic response. Wheat characteristics which affect the photoacoustic signal are density, thermal conductivity, specific heat, and optical absorption coefficient.

The modulated light beam was produced by a light emitting diode and the photoacoustic signal was detected with an electret microphone and a lock-in amplifier. Modulation frequency was in the range of 10-1000 Hz. In order to study structural differences between the two varieties transmission electron micrographs were taken and analyzed. Moisture absorption studies were carried out. Results of the moisture absorption studies help explain the structures observed in the micrographs.

Experiments were carried out using a typical hard and a typical soft variety of wheat and we were consistently able to differentiate between these two varieties on the basis of their photoacoustic response.